Delft University of Technology

Master's Thesis

Quantum Error Correction of Patch-Loss of the Surface Code

Author
S. Hu

Supervisor
D. Elkouss

April 5, 2020

Contents

3

Chapter 1

Introduction

Bell states

There are four maximally entangled two-qubit Bell states. Together, they form a maximally entangled basis known as the Bell basis.

$$|\phi^+\rangle = \frac{1}{2}\big(|00\rangle_{AB} + |11\rangle_{AB}\big) \tag{1.1}$$

$$|\phi^-\rangle = \frac{1}{2}\big(|00\rangle_{AB} - |11\rangle_{AB}\big) \tag{1.2}$$

$$|\psi^+\rangle = \frac{1}{2}\big(|01\rangle_{AB} + |10\rangle_{AB}\big) \tag{1.3}$$

$$|\psi^-\rangle = \frac{1}{2}\big(|01\rangle_{AB} - |10\rangle_{AB}\big) \tag{1.4}$$

The Bell state that we want to prepare, $|\phi^+\rangle$, can be created by applying the Hadamard and the CNOT gate on two qubits.
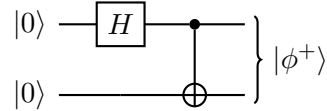
However, due to the fact that the system is imperfect, a Werner state will be created instead with fidelity F, which is given by the following density matrix,

$$\rho_W = F\,|\phi\rangle\langle\phi| + \frac{1-F}{3}\sum_{i=1,2,3}|\psi_i\rangle\langle\psi_i| \tag{1.5}$$

where $|\phi\rangle$ now represents the Bell pair that we want to prepare, and $|\psi_i\rangle$ are the other three Bell states. The production of this noisy Bell pair will be illustrated by
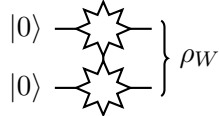
Single selection

Luckily, the fidelity of a noisy Bell pair can be enhanced through entanglement purification. In the process of *single selection*, a single noisy Bell pair is used (utility pair) in order to enhance the fidelity of another noisy bell pair (target pair). Here CZ gates are applied between the first and second qubits of the two noisy pairs. A successful parity check on the utility pair yields an enhanced target pair.
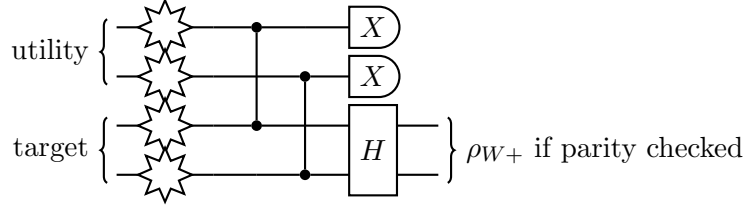
We should separate the qubits based on their location. Alice and Bob both holds one of the two qubits of both the utility and target pair. We put the qubits held by Alice on top, and Bob on the bottom.
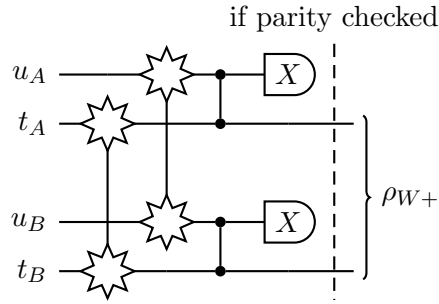
The enhanced Bell pair $\rho_{W,1}$ can be iteratively enhanced using the same scheme using newly created noisy Bell pairs ρ_W. After repeated iterations the fidelity will converge to some maximally attainable value, dependant on the fidelity of the noisy Bell pair. Two iterations of single selection is displayed below.
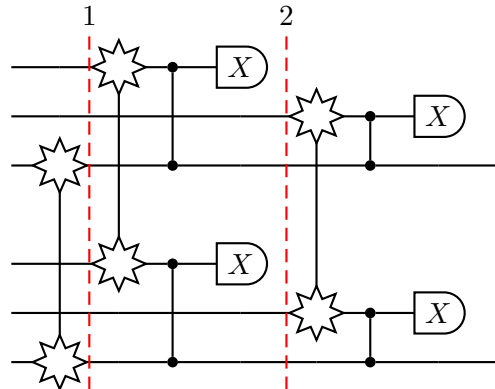
Entanglement pumping

Within each iteration, we can add additional *nested levels* to further improve the purification. In each nested level, we perform extra rounds of single selection, but taking two enhanced Bell pairs from the previous level as input. For example, in the first nested level, a Bell pair ρ_{W+} is used to purify another Bell pair with the same fidelity to ρ_{W++}, which will be the input state for the second nested level.

Double selection

Another approach which yields a higher enhanced fidelity utilizes two noisy Bell pairs ($u1$ and $u2$) to enhance a third pair (t). They perform a CZ gate locally between $u1$ and t, followed by another between $u2$ and $u1$. Now, they perform parity checks on $u1$ and $u2$. If both parity checks are passed, the protocol succeeds and the target qubit fidelity is enhanced.

6
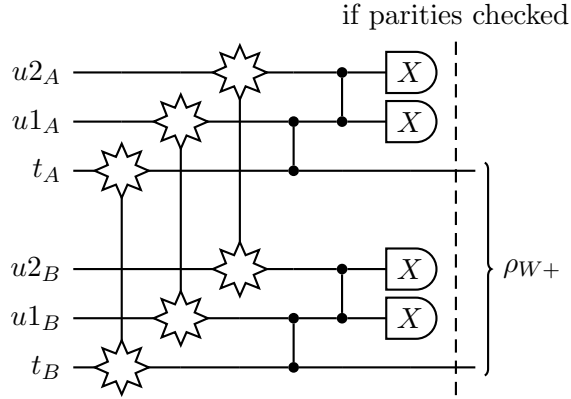
Chapter 2

Quantum error correction

To build a real world quantum computer, or a quantum communications device, one has to deal with the presence of noise, which will inevitably alter the quantum state of a qubit stored or passed through a communications channel. Recent developments have raised the fidelity of single qubit operations to up to one single failure in 10^6 operations [1]. But even this fidelity is not enough, as a full quantum computation may require millions of qubits, and the generation of entangled states over a large number of qubits. With imperfect quantum gates, anything we do in order to perform a computation will add to the error.

The theory of *quantum error correction* has been developed to counteract this noise, by using a larger number of redundant *physical qubits* to encode for a smaller number of *logical qubits*. By adding extra redundant qubits in our *error correcting code*, we can carefully encode the quantum state which we wish to protect, as long as the rate of errors on the physical errors is low enough [2, 3, 4].

In this chapter, we will introduce the principles of quantum error correction by the example of the *three-bit repetition code*. In section 2.1, we will first cover the classical variant, and the quantum variant in section 2.2. A more practical language to describe these codes is the *stabilizer formalism*, in section 2.3. The set of tools and principles explained in these sections form the basis for higher level quantum codes that we will come later in this thesis.

2.1 Classical three-bit repetition code

To introduce some of the terms that we are going to use later, let us first start with a classical example the three-bit repetition code. This code encodes bits (a single bit in the example) by repeating them. Let the *codewords* of the single logical bit be:

$$0_L = 000 \qquad\qquad 1_L = 111 \qquad\qquad (2.1)$$

In order to do computations, a NOT gate may be applied to the codewords to flip the logical value:

$$000 \leftrightarrow 111 \qquad\qquad (2.2)$$

A *bit-flip* error can occur on any of the three bits in the code, which flips the single bit-value from 0 to 1 and 1 to 0. An error can be *detected* by measuring the bits and comparing whether the bits have equal value. An detected error can be *corrected* by computing the majority-function of the bitstring. Thus the three-bit repetition code will be correctly corrected if less than half of the bits were flipped.

$$0_L \xrightarrow{E_2} 010 \xrightarrow{correction} 000 \qquad\qquad 0_L \xrightarrow{E_2,E_3} 011 \xrightarrow{correction} 111 \qquad (2.3)$$

The *distance d* of a classical code is the minimum amount of bit flips to transfer one codeword to another. In the case of the three-bit repetition code, the code distance is 3. The number of bits in de code n, the number of encoded bits k and the distance of a code can be used to fully describe a code in the $[n, k, d]$ notation. The three-bit repetition code is a $[3, 1, 3]$ code.

2.2 Quantum three-bit repetition code

From here, we can describe how to do computations on a quantum system. We start by considering an example of the *quantum three-bit repetition code*, where the classical bits are now replaced by qubits that can be in the superposition of the two classical 0 or 1 states. The basis states of the encoded qubit is the tensor product of the single qubit states:

$$|0\rangle_L = |0\rangle \otimes |0\rangle \otimes |0\rangle = |000\rangle \qquad |1\rangle_L = |1\rangle \otimes |1\rangle \otimes |1\rangle = |111\rangle \qquad (2.4)$$

A pure qubit state can also be a superposition of the bases states and is encoded as:

$$|\psi\rangle_L = \alpha |0\rangle_L + \beta |1\rangle_L \qquad (2.5)$$

2.2.1 Pauli operators

The Pauli operations are unitary operations on single qubits, and will be applied very often throughout this thesis. Including the identity operator, the Pauli group on a single qubit, $\mathcal{P}_1$, consists of:

$$X = \begin{bmatrix} 0 & 1 \\ 1 & 0 \end{bmatrix} \qquad Y = \begin{bmatrix} 0 & -i \\ i & 0 \end{bmatrix} \qquad Z = \begin{bmatrix} 1 & 0 \\ 0 & -1 \end{bmatrix} \qquad I = \begin{bmatrix} 1 & 0 \\ 0 & 1 \end{bmatrix} \qquad (2.6)$$

The Pauli operators represent errors that can occur on a single qubit. The Pauli X operator is analogous to the classical *bit-flip* error and acts on the qubit computational basis states:

$$X |0\rangle = |1\rangle \qquad\qquad X |1\rangle = |0\rangle \qquad (2.7)$$

Additionally, the Pauli Z operator introduces phase errors on a quantum bit:

$$Z |0\rangle = - |0\rangle \qquad\qquad Z |1\rangle = - |1\rangle \qquad (2.8)$$

The elements of the Pauli group on n qubits, $\mathcal{P}_n$, consists of tensor products of single qubit Pauli operators, such that $\mathcal{P}_n = \mathcal{P}_1^{\otimes n}$. We use the index of a Pauli operator to indicated on which qubit it has operated on, while other qubits are acted on by the identify. In cases without indices, the order of the operators indicate the qubit it acts on. For example, element $P = X_1 \otimes X_2 = XX$ on the three-bit repetition code means that qubit 1 and 2 have been acted on by the Pauli X operator, while qubit 3 is acted on by the identity. The tensor product symbol is often omitted for clarity, such that the above operation can be also written as $P = X_1 X_2$. The *weight* of an operator is the number of qubits on which it does not act non-trivially. On the pure three-qubit encoded state, a bit-flip error on the second qubit is applied as:

$$X_2 \left| \psi \right\rangle_L = (I \otimes X \otimes I) \left| \psi \right\rangle_L = \alpha \left| 010 \right\rangle + \beta \left| 101 \right\rangle \tag{2.9}$$

2.2.2 Logical operations

In order to do computations on the encoded qubit of our three-bit repetition code, we wish to find the Pauli operators in $\mathcal{P}_3$ which flips any basis of the basis states of the encoded qubit to the other. We find that $X \otimes X \otimes X$ transforms $\left| 0 \right\rangle_L$ to $\left| 1 \right\rangle_L$, which is known as the logical bit-flip.

Furthermore, we now have the logical Z operator which must map $\left| 0 \right\rangle_L$ to $-\left| 0 \right\rangle_L$ and $\left| 1 \right\rangle_L$ to $-\left| 1 \right\rangle_L$. We see that for example $Z \otimes I \otimes I$ achieves this, but also any other $\mathcal{P}_3$ operator with two identities and one Pauli Z operator. Thus there are multiple operators that achieves the same. We formalize the logical operators as

$$\bar{X} = XXX \qquad\qquad \bar{Z} = ZII \tag{2.10}$$

The distance of a quantum code is the minimal weight of any logical operators on the code. In the above case, the weight of the encoded X operator $\bar{X}$ is 3, hence the code can detect up to 2 X errors, analogous to the classical case. However, the weight of the encoded Z operator $\bar{Z}$ is only 1, which means that Z errors cannot be detected at all.

2.2.3 Error detection

To detect errors in our repetition code, we now cannot measure the states directly, as any measurement would collapse the encoded state, and therefore destroy the encoded information. Instead, we can now detect errors by measuring the *parity* of two or more qubits rather than single qubits. For example, for two qubits, we can measure the parity by adding an *ancillary* or *ancilla* qubit prepared in $\left| 0 \right\rangle$ and measure it in the computational basis after connecting our quantum circuit as:

Note that measuring the ancilla qubit in the computational basis will be equivalent to measuring $Z \otimes Z$ on the first two qubits, as

$$
\begin{aligned}
(ZZ) \left| 00 \right\rangle &= \left| 00 \right\rangle & (ZZ) \left| 01 \right\rangle &= -\left| 01 \right\rangle \\
(ZZ) \left| 10 \right\rangle &= -\left| 10 \right\rangle & (ZZ) \left| 11 \right\rangle &= \left| 11 \right\rangle
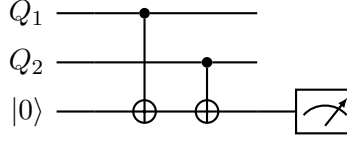\end{aligned}
\tag{2.11}
$$

Figure 2.1: The quantum circuit for a parity measurement on two qubits, Q_1 and Q_2, which is measured on the ancilla qubit prepared in $|0\rangle$.

Now for our quantum three-bit repetition code, we need to setup ancilla qubits between each of the 3 qubits, such that the parity between any two qubits can be measured. For the state in equation 2.5, any parity measurement ZZI, ZIZ or IZZ will return even parity. If one of the qubits has encountered a bit-flip error such as in the second qubit in equation 2.9, two of the parity measurements will return a -1 eigenvalue, in this case ZZI and IZZ.

Furthermore, we see that no configuration of ancilla qubits could be set up for the three-bit repetition code to detect for phase errors, which was already set by the weight of the logical Z operator.

2.2.4   Error correction

As the error has been identified, we can apply correct Pauli operator from $\mathcal{P}_3$ to correct the error. In the above case, we wish to apply IXI to clip the second qubit to correct the code.

In the quantum three-bit repetition code, we can very simply deduct which qubit has encountered an error from the combination of uneven parity measurements. This is called *decoding* the error and is the main function of a *decoder*. More complex error correcting codes involves decoding algorithms which are far more complex than in the three-bit repetition code, which we will see more of later.

2.3   Stabilizer Formalism

As we have seen above, we can use the Pauli group $\mathcal{P}_n$ to easily describe a quantum error correcting code of n qubits, without explicitly looking at the *state* of the qubit. This powerful technique is called the *stabilizer formalism* [5], and is the most widely formalism used to describe topological codes.

A quantum error correcting code that can be described using the stabilizer formalism is called a *stabilizer code*. A stabilizer code is defined by two sets of operators, a set of *stabilizer generators* which form the *stabilizer group* $\mathcal{S}$, which is an Abelian subgroup of the Pauli group, and a set of encoded *logical operators*. A stabilizer group is the set of Pauli operators which leave all states $|\psi\rangle_i$ from the *codespace*, a subspace of the Hilbert space of n qubits spanned by the codeword basis states, invariant, such that:

$$S |\psi\rangle_i = |\psi\rangle_i, \qquad\qquad \forall S \in \mathcal{S} \tag{2.12}$$

These elements of the of the stabilizer group are most simply referred to as *stabilizers*. The elements of this Abelian group can be written by a set of independent generators S_j of size N_S, where any stabilizer S can be written as

$$\mathcal{S} = \prod_j S_j^{a_j}, \qquad\qquad a_{\_j} \in 0,1 \qquad\qquad (2.13)$$

The set of generators S_j is *independent* if no generator can be written as a product of other generators. This implies that any stabilizer can be written in terms of the bitstring $a_1, a_2, ...a_{N_S}$ and that the stabilizer group takes up n_S degrees of freedom of the Hilbert space of N qubits. The remaining $N - N_S = N_L$ degrees of freedom which are not specified by the stabilizers make up the *codespace*, the subspace spanned by the logical basis states, or the number of encoded logical qubits. Thus, if N_L logical qubits are to be encoded by n qubits, we require a total of $N_S = N - N_L$ independent stabilizer generators.

2.3.1 Encoded logical operators

Next to the set of stabilizers, we can construct the set of logical operators that will act on the encoded qubits from a set commutation rules. First of all, all logical operators must commute with all elements of the stabilizers, as a logical operator is made up from Pauli operators, and any Pauli operator which anticommutes with a stabilizer cannot leave the codespace invariant. Note that his means that a logical operator is not unique, as it can be multiplied with an element of the stabilizer. Secondly, we can impose commutation rules for the logical operators themselves based on the Pauli operators that they are representing. For example, logical $\bar{X}$ and $\bar{Z}$ operators must anticommute.

The minimum weight of the logical operator determines the distance d of the error correcting code. This is thus the minimal amount of errors that can cause a logical failure. Together with the total number of qubits n and number of logical qubits k, they provide a rough measure of the error correcting capabilities of the code.

2.3.2 Error detection procedure

As the stabilizers are a set of Pauli operators, they correspond to blip-flip or phase-flip errors that may have happened on any of our n qubits. Furthermore, as any stabilizer leaves all states $|\psi\rangle_i$ invariant, measuring the stabilizers does not disrupt the encoded information. If no error has occurred, all stabilizer measurements will return a '+1' eigenvalue, while any '-1' outcome points to the presence of errors, which we will call a *stabilizer violation*.

This outcome is dependent on whether an error caused by the error operator E, must either commute or anticommute with the stabilizer generators, since all operators are members of the same Pauli group $\mathcal{P}_n$. If E and generator S_j commute then,

$$S_j E |\psi\rangle = E S_j |\psi\rangle = E |\psi\rangle \qquad\qquad (2.14)$$

which means that the post-error state is a +1 eigenstate of S_j. If E and generator S_j anticommute then,

$$S_j E |\psi\rangle = -E S_j |\psi\rangle = -E |\psi\rangle \qquad\qquad (2.15)$$

and the post-error state is a -1 eigenstate of S_j. Errors on stabilizers codes are therefore detected by measuring the stabilizers, which returns a series of eigenvalue outcomes that is called the *syndrome*. However, it is not necessary to measure all operators in the stabilizer group $\mathcal{S}$. Measuring the set of independent stabilizer generators S_j suffices as any other stabilizer is just a combination of already measured states.

2.3.3 Error models

Any qubit can be subject to a combination of errors, each can be caused by a difference factor in our quantum system. To generalize these errors, we define certain *error models* that constricts the errors that take place. Here, we list a few models that we will encounter in this thesis.

Independent noise model We were already introduced in the *bit-flip* and *phase-flip* errors in section 2.2.1. But let us know generalized them in the form of the density matrix ρ. Let Φ be a quantum channel that maps ρ to $\Phi(\rho)$, and let the chance of a bit-flip error be p_X, the resulting state should be

$$\Phi_X(\rho) = (1 - p_X)\rho + p_X(X\rho X). \tag{2.16}$$

Analogously, let the chance of a phase-flip error be p_Z, the resulting state should be

$$\Phi_Z(\rho) = (1 - p_Z)\rho + p_Z(Z\rho Z). \tag{2.17}$$

The bit-flip and phase-flip errors can be considered together as the *independent noise model* or the *uncorrelated noise model*. As the two types of errors are independent, they can be studied separately from each other.

The depolarizing noise model In the *depolarizing* noise model, the afflicted quantum state is replaced by a complete mixed state with probability p_D. Let the completely mixed state be written as

$$\frac{1}{2}I = \frac{1}{2}(\rho + X\rho X + Y\rho Y + Z\rho Z), \tag{2.18}$$

then the depolarizing channel is described as

$$\Phi_D(\rho) = (1 - \frac{3}{4}p_D)\rho + \frac{p_D}{4}(X\rho X + Y\rho Y + Z\rho Z) \tag{2.19}$$

$$= (1 - p_D^*)\rho + \frac{p_D^*}{3}(X\rho X + Y\rho Y + Z\rho Z) \tag{2.20}$$

which can be interpreted as the state ρ is left untouched with probability $p_D^* = \frac{3}{4}p_D$, and each Pauli gate is applied to it with probability $1 - p_D^*$. Differently from the *independent noise model*, to optimally decode, we need to take into account correlations between X and Z errors.

The erasure noise model   In the *erasure* noise model, a qubit is completely erased or lost from the system. Such a loss can be detected and the missing qubit is then replaced by a qubit in the totally mixed state (equation 2.18). The erasure channel can therefore be seen as the depolarizing channel with the extra property that it can be detected which qubits suffer the error.

2.3.4   Error correction or decoding

As the Pauli operators are self-inverse, any error E can be corrected by applying it again. From the measurement outcomes of a stabilizer measurement, we can deduce which error E must have caused the syndrome. However, this relationship is not always one-to-one, as an error E and its multiplication with a stabilizer ES will lead to an identical syndrome. This is called the *code degeneracy*. The choice of the most appropriate error to correct is not a trivial task, and algorithms that are tasked to automate this process are called *decoders*.

2.3.5   Stabilizer codes

The three-qubit repetition code we already covered can now be described in the stabilizer formalism. We had already found that the logical operators are encoded $\bar{X} = XXX$ and $\bar{Z} = ZII$. Other logical operators also exist up to a stabilizer. The stabilizer generators are needed to complete its description. We had found that two parity measurements, for example ZZI and IZZ, will identify the error, as they will either commute or anticommute with the error, as such they are a set of independent stabilizer generators.

The resulting measurement of '+1' or '-1' eigenvalues make up the syndrome. De decoder algorithm here is quite simple, but fails in the case if there is more than 1 bit-flip error. The code has $n = 3$ and $n_S = 2$ which results in the expected $n_L = 1$ encoded bits. The distance d of the is 1, which conforms that there are certain errors, in this case phase-flip errors, which this code cannot detect.

The smallest code which can correctly solve for both single bit-flip and phase-flip errors is the *5-qubit repetition code* [6]. This code has the following stabilizer generators:

$$XZZXI \qquad IXZZX \qquad XIXZZ \qquad ZXIXZ \qquad (2.21)$$

with the logical operators up to a stabilizer:

$$\bar{X} = XXXXX \qquad\qquad \bar{Z} = ZIIII \qquad (2.22)$$

This codes now has $n = 5$ bits with $n_S = 4$ stabilizers, which means it still encodes for a single bit.

With the principles of encoding and decoding in the quantum error correction in mind, we are now ready to move on to a more complicated variant of stabilizer codes, the *surface code*.

13

Chapter 3

The surface code
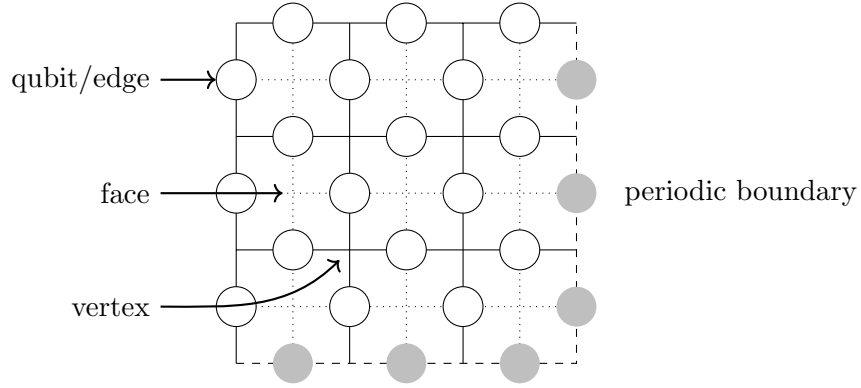
Figure 3.1: The toric code is defined as a $L \times L$ lattice (here $L = 3$) with periodic boundary conditions. The edges on the lattice, which represents the qubits, make up faces and vertices.

The variant of the stabilizer codes that we are going to explore in this thesis is Kitaev's *surface code* [7], which is of the category of *topological codes*. Among this category, the surface code is preferable as it offers the highest error tolerance under realise noise channels and requires only local stabilizer measurements of physically neighboring qubits. Two variants of the surface code will be considered here, the *toric code* in section 3.1 and the *planar code* in section 3.2, and various decoders are detailed in 3.3.

3.1   The toric code

The *toric code* is defined by arranging qubits on the edges of a square lattice with periodic boundary conditions, as seen in Figure 3.1. The name of the toric code lends itself from the torus, or donut, shape, where any point on the surface of the torus will encounter itself after traversing the torus in either x or y directions. Hence, the top edge of the toric code meets the bottom edge, whereas the left edge meets the right. On a $L \times L$ grid there are $N = 2L^2$
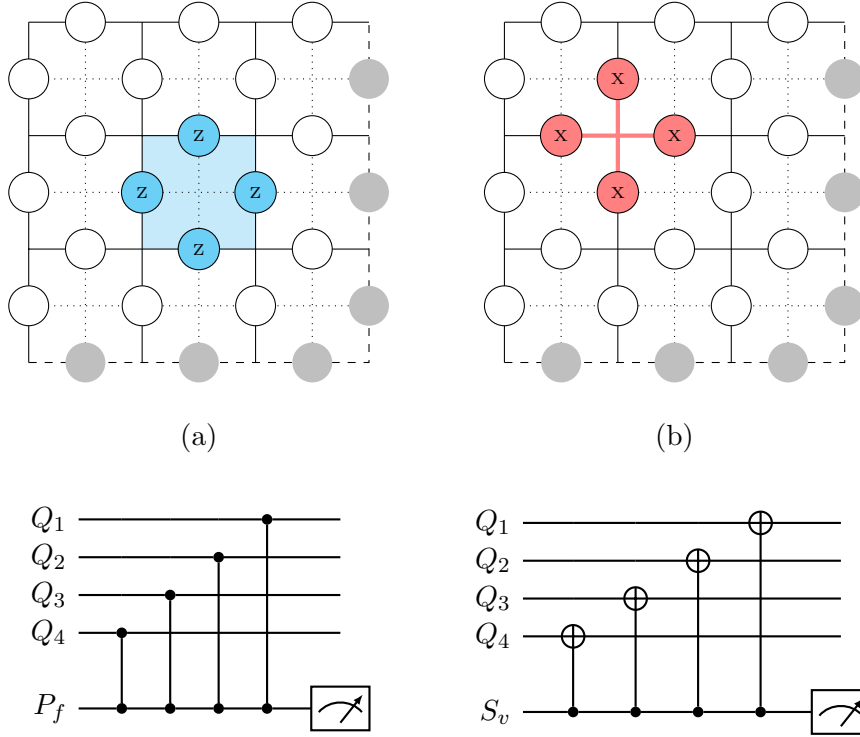
Figure 3.2: Each face (a) and vertex (b) on the lattice represents a plaquette and star oper-ator, respectively. The non-identity single qubit operators on which they act are indicated. The set of all (but one) plaquettes and vertices make up the stabilizers of the code.

edges and the same amount of physical qubits. This topology of qubit arrangement plays an important part in encoding the logical qubits, which is stored in the non-trivial cycles on the torus. Errors, beneath a certain threshold, will only introduce local effects and does not change these cycles.

3.1.1 Stabilizer generators

To define a stabilizer code, we need to specify the m independent stabilizer generators and the encoded $\bar{X}$ and $\bar{Z}$ operators. On the toric code there are two types of stabilizer generators, *plaquette* and *star* operators, which are associated with the *faces* and *vertices* of the square lattice, respectively.

Plaquette operators   For every face f on our lattice, we define a plaquette operator P_f, consisting of tensor product of Pauli Z operators on qubits on these edges (see Figure 3.1a),

$$P_f = \bigotimes_{i \in Q(f)} Z_i \tag{3.1}$$

15

where $Q(f)$ is the set of qubits touching face f. On a $L \times L$ grid there are L^2 plaquettes.

Star operators Similarly, for every vertex v on our lattice, we define a star operator S_v, consisting of tensor product of Pauli X operators on qubits neighboring the vertex (see Figure 3.1b),

$$S_v = \bigotimes_{i \in Q(v)} X_i \tag{3.2}$$

where $Q(v)$ is the set of qubits neighboring vertex v. On a $L \times L$ grid there are L^2 plaquettes.

As each plaquette and star operator needs to be measured, an ancilla qubit is needed at the physical locations of each of these operators. The structure of the full lattice is now clear, as it just a simple square arrangement of alternating data and ancilla qubits in both x and y directions.

The full stabilizer of the code $\mathcal{S}$ can be generated by multiplying elements of the generator operators. Consider two plaquette operators. These two operators will either share one boundary consisting of a qubit, or none. This means that the Pauli Z operator on the boundary qubit will add up to identity as they commute. The result is that the product of the plaquette operators will consists of the overall boundary Pauli operators of the joint plaquette (see Figure 3.3a).

However, if all plaquettes are applied to the lattice, no boundary will be left. Thus the product of all plaquettes is the identity, which means that the full set of plaquettes are not independent. The full set of plaquette generators can therefore be completed by simply removing a single plaquette from all available plaquettes. There are therefore $L^2 - 1$ independent plaquette operators.

The multiplication of star operators follow the same properties as the plaquette operators described above (see Figure 3.3b). Thus there are also $L^2 - 1$ independent star operators, which are the star generators. This sums up to $N_S = 2L^2 - 2$ independent stabilizer generators.

3.1.2 Dual lattice

Note that if we shift our lattice half a cell down, and half a cell to the right, we can create a *dual* lattice. This dual lattice has the same size and same boundary conditions as the *primal* lattice, but every plaquette in the primal lattice is a star in the dual lattice, and every star in the primal lattice is a plaquette in the dual lattice. The edges of the dual lattice are plotted with dotted lines in the figures.

This interesting property of *lattice duality* leads to the fact that plaquette and star operators are in fact the same, and we can choose from either that is best suited for the calculation. The multiplication of operators is best pictured in the plaquette picture, for example. For the square lattice in the toric code, the dual lattice is coincidentally also square. For other types of topological codes with non-square lattices, the dual lattice has a different lattice structure than the primal lattice. We will not explore these kind of lattices in this thesis.
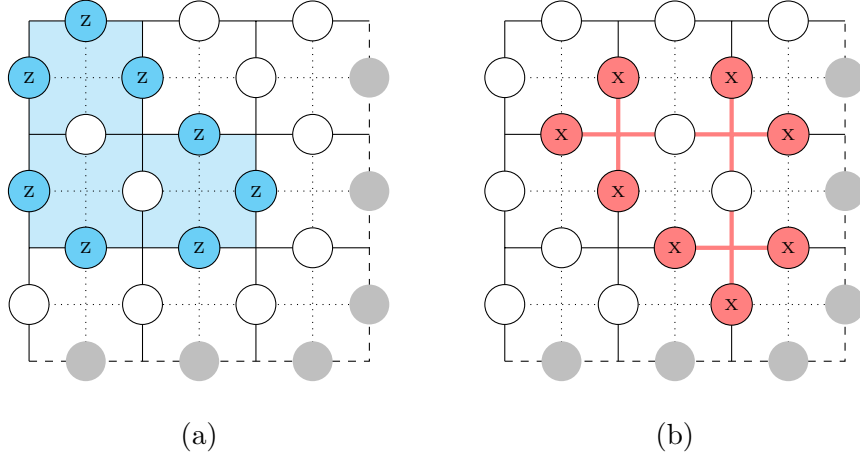
Figure 3.3: Multiplication of (a) plaquette and (b) star operators will result in a operator that consists of the Pauli operators that reside on the overall boundary of the joint plaquettes or stars.

3.1.3 Encoded qubits

Since there are $N = L^2$ qubits and $N_S = 2L^2 - 2$ independent stabilizers, we must have $N_L = N - N_S = 2$ encoded qubits and therefore 4 logical operators $\bar{X}_1, \bar{X}_2, \bar{Z}_1$ and $\bar{Z}_2$.

Recall the logical operators consists of the Pauli operators, and must commute with all stabilizer generators, but cannot be part of the stabilizer itself. We can construct the logical operators by starting with, for example, a single Pauli Z operator. It commutes with all plaquette operators trivially. In terms of the star operators, this single Pauli Z operator commutes with all but the two neighboring qubits, as all others apply to different qubits. Adding another Pauli Z operator will shift will of the anticommuting neighboring star operators. We know see that a closed loop of Z operators around the torus does not have neighboring star operators, and therefore commute with all stabilizers. As the torus has two directions we can loop over, these are the logical $\bar{Z}$ operators (see Figure 3.4a-b). Analogously, we can construct the logical $\bar{X}$ operators in the same way (Figure 3.4c-d).

Note that these logical operators are not unique. As the logical operators commute with the stabilizers, these $\bar{X}$ and $\bar{Z}$ operators can be multiplied with e.g. a plaquette or star operator, respectively, which create a diversion from its original path. But as the path still loops around the torus, this is still a valid logical operator.

The logical operators have a minimum length of L qubits, which is also the distance of the toric code. The toric code is therefore a $[L^2, 2, L]$ in the [n,k,d] notation. This implies that the toric code might be more robust against errors if the size of the lattice is increased. Later we will see that this is also very much dependent on the type of decoder that is used, and that different decoders will lead to different regimes of error for which this reasoning is true.
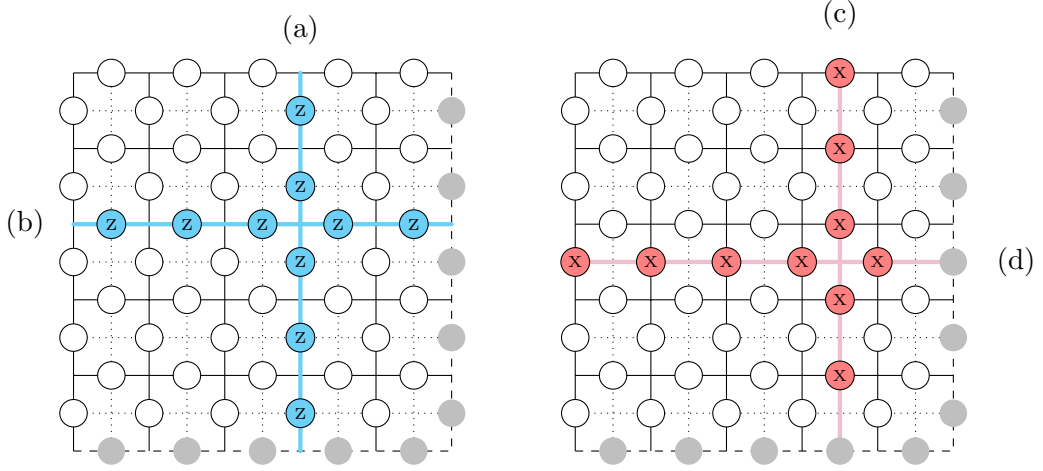
Figure 3.4: The logical (a) $\bar{X}_1$, (b) $\bar{X}_2$, (c) $\bar{Z}_1$ and (d) $\bar{Z}_2$ operators are the closed loop of X and Z operators, respectively, that go around the two boundaries of the torus.

3.1.4 Error detection

As discussed in the previous chapter, errors are detected by measuring the set of stabilizer generators. As we have seen in the previous section, this consists of all but one plaquette operators P_f and all but one star operators S_v. Let us first consider to measure all of them.

In the case of a single Z error (Fig 3.5a.i), the neighboring plaquette operators will commute with this error, as it consists of Pauli Z operators itself. But the neighboring star operators anticommutes with this error according to equation 2.15. Similarly, a single X error (Fig 3.5a.ii) commutes with neighboring star operators but anticommutes with neighboring plaquette operators. A Y error is a combination of X and Z operators and therefore anticommutes with all neighboring generator operators (Fig 3.5a.iii).

In the case of two Z errors (Fig 3.5a.iv), the star operators between the two errors now commute with the errors, creating a virtual path between them. This is a general property: given any string of errors, the generator operators at the end of the string will anticommute with the errors and measure -1. For Z errors, star operators at the end of strings on the primal lattice will measure -1. The detection of X errors occur in the same way, albeit now the strings of errors is defined on the *dual* lattice, and plaquette errors will measure -1 at the end of these strings.

Since Z and X errors independently affect different types of stabilizer measurements (stars and plaquettes, respectively), these two types of errors can be considered independently in two error correction processes. The two processes are analogous, up to the duality of the lattice. Therefore, for the remainder of the section, only Z errors, which leave a string of errors on the primal lattice, will be considered.
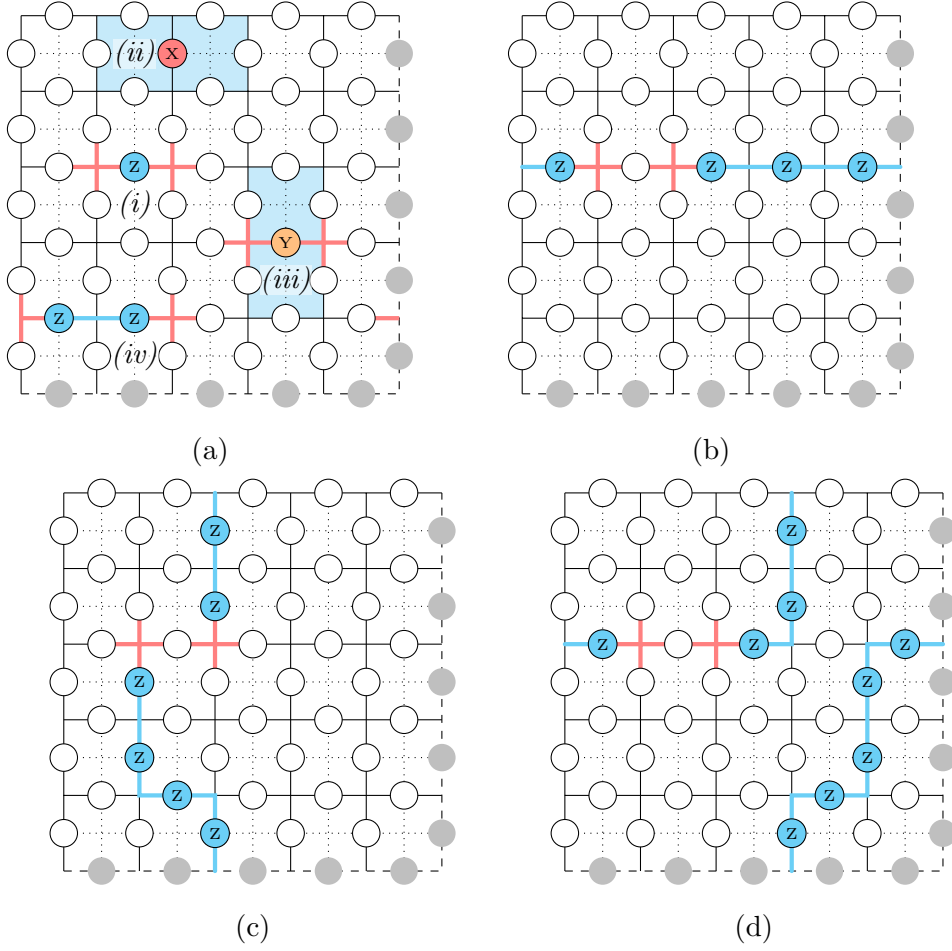
Figure 3.5: (a) Stabilizer generators that anticommute with the error will measure -1, which are (i) the neighboring star operators for a Z error, (ii) the neighboring plaquette operators for an X error, and (iii) both star and plaquette operators for a Y error. In the case of a string of errors (iv), only the stabilizer generators at the end of these strings will anticommute with the error. Due to code degeneracy, the single Z error in (a.i) E has the syndrome as (b) $E\bar{Z}_1$, (c) $E\bar{Z}_2$ and (d) $E\bar{Z}_1\bar{Z}_2$.

3.1.5 Error correction

An error E can be corrected by applying it again to the lattice. The error operator E is however unknown. We must therefore try to identify the correct operator given the measured syndrome. As mentioned in the previous chapter, this relationship between error does not always map one-to-one, which it is not in the surface code. An error E can be multiplied with some operator L that commutes with the stabilizer and they will result in the same syndrome.

If L is in the stabilizer $\mathcal{S}$, the product of the identified correction operator $C = E'$ with the real error operator E will leave the code invariant. The resulting operator $CE = L$ is a stabilizer operator. However, the encoded logical operators also commute with the stabilizer, which means that E, $E\bar{Z}_1$, $E\bar{Z}_2$, $E\bar{Z}_1\bar{Z}_2$ will all lead to the same syndrome (Fig 3.5a-d). Any identified correction operator C can therefore be categorised into four classes of operators, of which only one includes the correct logical operator. The task of choosing most appropriate correction chain is up to the decoders (section 3.3).

3.1.6 Quasiparticle picture

The processes of error detection and correction can alternatively be presented in the *quasiparticle picture*, where the anticommuting stabilizer measurements act like excitations on the lattice, which behave like the quasiparticles *anyons*. A single error creates a pair of anyons, and a chain of errors causes movement of the anyon on the lattice. A pair of anyons can also annihilate each other when two error chains merge. The correction of errors can thus be viewed of movement of the correction chains until all anyons are annihilated. The quasiparticle picture removes the distracting underlying lattice from the problem, and decoding becomes simply identifying the right pairing between anyons to minimize the chance of a logical error.
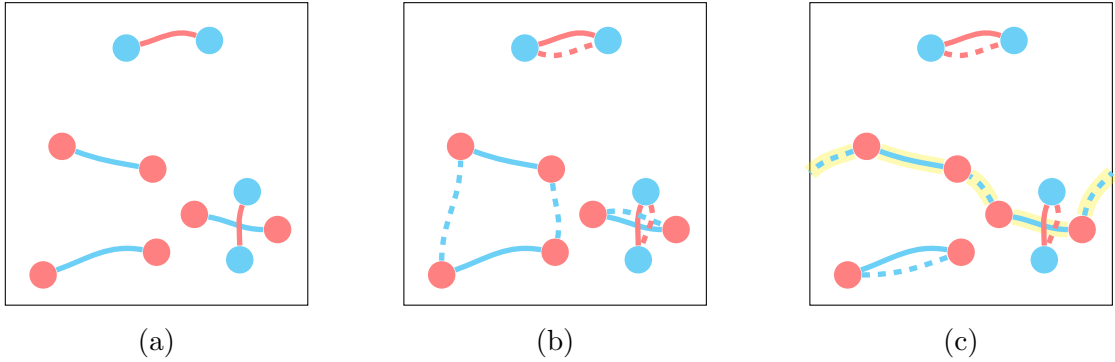

(a) (b) (c)

Figure 3.6: The quasiparticle picture of stabilizer measurements. Anticommuting stabilizers behave as anyons (circles), where a chain of errors (lines) creates a pair of anyons. Figure (b) shows a successful decoding of (a). Figure (c) shows a pairing that resulted in a correction operator that is in a different class as the error operator, which acquires a logical error.

Figure 3.6a shows the quasiparticle representation of the errors suffered in Figure 3.5a, which has suffered Z (blue lines) and X errors (red lines). The corresponding anyons can either be of the star type (red circle) or plaquette type (blue circle). Figure 3.6b shows a successful decoding. Note that here not all pairs are correctly identified, but the resulting loop still is in the same class of operators. In figure 3.6c the correction has failed as the resulting loop in the correction is in a difference class compared to the error. As the loop still commutes with the stabilizer, no error can be detected, but the encoded qubit has acquired a logical error.

3.1.7   Code threshold

Since the distance d of the toric code on a $L \times L$ is L, we would expect that we can improve the robustness of the code by increasing the lattice size L. However, this also increases the total number of errors in the lattice, that adds an increased level of complexity in choosing the correct correction operator.

In practice, there is a trade-off between the positive effect of a larger code distance and the negative effect of larger number of errors. When the error rate p is low, the positive effect outweighs the negative and increasing the lattice L will increase the probability of successful error correction p_C. When the error rate is large, the negative effect outweighs the positive and increasing p will decrease p_C. The point of transition in the error rate is called the *code threshold* p_{th}.

The code threshold is not the only parameter that determines the potential of a certain code for practical use. The behavior for error rates far below the threshold is also important, as is the number of physical qubits needed to achieve the sought after level of error suppression. Nevertheless, the code threshold provides us with a very easy and useful tool to benchmark different codes and different decoding algorithms, and to compare them with each other. Therefore, in this thesis we will heavily rely on the value of the code threshold. The value of the threshold is heavily dependent on the chosen error model and the physical conditions of the stabilizer measurements. To compare different decoding algorithms, we therefore will use independent and identically distributed errors (i.i.d. noise), which is the *independent noise model* from section 2.3.3.

For the toric code, when the only source of errors is i.i.d. noise under the independent noise model, and all measurements can be made perfectly, the *optimal threshold* has been proven to be 10.9% (see section 3.3.1). However, to achieve this value, one needs to consider all possible error configurations on the lattice to identify the correction operator C that is most likely to be equal to the error operator E. This is a computationally heavy task that scales exponentially with the lattice size. It is therefore an impractical approach in reality.

Luckily, there exists other decoding algorithms that can find a solution much faster, albeit at the cost of reducing the code threshold. Edmond's *Minimum Weight Perfect Matching* (MWPM) decoder scales cubic with the system, which allows for faster decoding, and achieves a code threshold of 10.3% (section 3.3.2). Including faulty measurements the threshold drops down to 2.9%. The *Union-Find* decoder is a relatively new addition to the set of decoders for the surface code. It scales *almost* linearly with the system, and

has a code threshold of 9.9% (section 3.3.3). In this thesis, we will try to combine certain properties of different decoders. In particular, we have created a heuristic for minimum weight which can be applied to the Union-Find decoder.

3.2 The planar code

Another variant of the surface code is the *planar code*, which disposes the periodic boundary conditions of the torus. This allows the qubits to be placed onto a flat 2D surface. For real systems in which the qubits physically interact with each other, this is a huge benefit. Therefore, in this thesis, we will consider both toric and planar variants of the surface code.
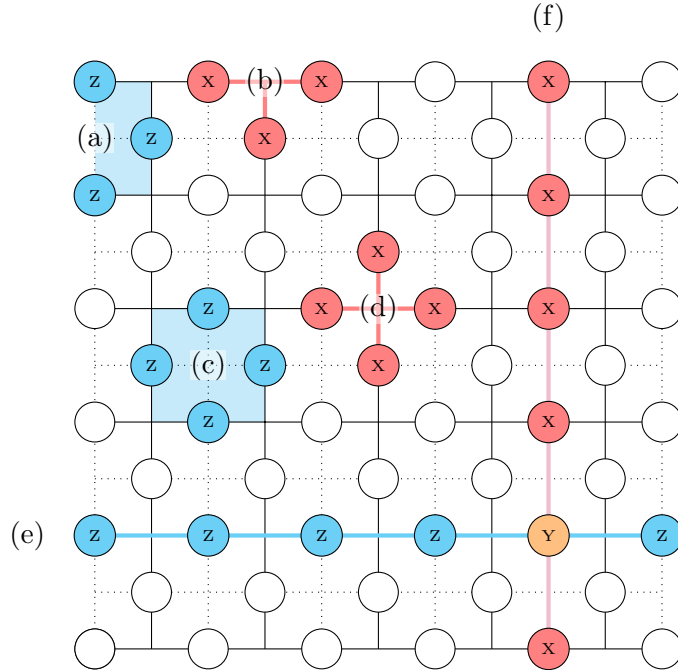
Figure 3.7: The planar code with lattice size $L = 4$, which includes $N = 2L^2 - 2L + 1$ qubits and $N_S = 2L^2 - 2L$ independent stabilizers. The boundary is defined by the (a) EDGE-plaquette and (b) EDGE-star operators, which exist next to the known (c) plaquette and (d) star operators, similar to the toric code. The planar codes encodes 1 logical qubit, which is represented by the logical (e) $\bar{Z}$ and (f) $\bar{X}$ operators.

Stabilizer generators There are a few key differences between the planar and toric codes. First of all, a new type of stabilizer generators define the non-periodic boundary of the lattice, which are referred to as *EDGE operators*. These EDGE operators have only 3 neighboring qubits and are therefore the tensor product of 3 Pauli operators. The EDGE-plaquette operators lie at the east and west boundaries of the lattice (Figure 3.7a) and

the EDGE-star S_{vE} operators lie at the north and south boundaries of the lattice (Figure 3.7b). In the middle of the lattice, the bulk of the stabilizer generators still consist of 4 Pauli operators, identical to the ones in the toric code (Figure 3.7c-d). Note that the stabilizer generators are still defined by equation 3.1 and 3.2, but now the relevant faces and vertices contain three neighboring qubits.

Stabilizer viloations A second key difference is that now not all errors will cause two stabilizer violations. In the bulk of the qubits on the lattice, a single error will still cause two neighboring stabilizers to measure -1, or create two anyons. At the boundary however, it now may be the case that an error is only included in one plaquette or star operator. This will also mean the decoding in the quasiparticle picture requires a slightly different approach.

Logical qubits Furthermore, we can inspect that a planar surface of dimension L has $N = 2L^2 - 2L + 1$ physical qubits. We can also find that there are $2L^2 - 2L$ stabilizer generators. As the boundary is now non-periodic, all generators are now independent, and therefore the number independent generators is $N_S = 2L^2 - 2L$. This means that the planar code encodes $N_L = N - N_S = 1$ a single logical qubit. The logical $\bar{X}$ and $\bar{Z}$ operators are pictured in Figure 3.7e-f.

Other properties of the planar code are very similar to the toric code. The *dual lattice* also exists for the planar code, for example. But the dual lattice exists at a 90 angle compared to the primary lattice. Also, as the bulk of the lattice still consists of 4-Pauli operator stabilizers, the decoding algorithms for the planar code is very similar to the toric code. It is due to the boundary that some slight alterations are needed, as we will see in the next section.

3.3 Decoders

3.3.1 The optimal decoder

3.3.2 Minimum Weight Perfect Matching

3.3.3 The Union-Find decoder

Even the fastest MWPM algorithms still have a quadratic time complexity of $\mathcal{O}(n^2\sqrt{n})$, where n is the number of qubits. In order to realistically utilize a decoder with increasing decoding success rates using increasing lattice size, we would need to have a better time complexity. Luckily, an alternative algorithm called the Peeling Decoder has been developed which can solve errors over the erasure channel with a linear time complexity $\mathcal{O}(n)$ [8]. The Union-Find Decoder builds on top of the Peeling Decoder to solve for Pauli errors with a time complexity of $\mathcal{O}(n\alpha(n))$, where α is an inverse Ackermann function, which is smaller

than 3 for any practical input size [9]. However, these algorithms have a tradeoff in the form of a decrease in the error threshold, and has the reported value of $p_{UF} = 9.2\%$.

A topic of interest will be weighted growth function for the Union-find decoder. This function of the algorithm will increase the error threshold to $p_{UF} = 9.9\%$, but has not been fully described in its publication. In this section, we will describe the original Peeling decoder and the Union-Find decoder.

The Peeling decoder

Let $\varepsilon \subset E$ be an erasure, a set of qubits on which an erasure error occurs, and let $\sigma \subset S$ be the measured error syndrome, the subset of stabilizer generators which anticommute with the erasure errors. In the absence of Pauli errors, all errors P must lie inside the erasure. Therefore, for any pair of stabilizer generators in σ, the path of errors must also be in the erasure, which can be denoted by $P \subset \varepsilon$. Furthermore, due to the fact that errors P are randomly distributed, any coset of errors and stabilizers $P \cdot S$ that solves the error syndrome σ is the most likely coset. These features of an erasures forms the basis of the Peeling decoder. In order to find a coset of $P \cdot S$, the decoder reduces the size of the erasure by peeling edges from the erasure, while keeping the syndromes at the new boundary of the erasure. Elements of the syndrome can be moved by applying an correction on the adjacent qubit. At the end, the entire erasure is peeled or removed, and all corrections will have removed the errors up to a stabilizer.

> use capitals for sets Σ, and lowercase σ for elements in the set

We will now describe the Peeling decoder as is presented in Algorithm 1. In step 1, we will remove all cycles present in ε. We construct a spanning forest F_ε inside erasure ε, the maximal subsect of edges of ε that contains no cycles and spans all vertices of ε. From here, we loop over all edges in F_ε (step 3), starting at a leaf edge $e = \{u, v\}$, removing the leaf edge from F_ε (step 4), and conditionally add the edge to the correction set κ if the pendant vertex u is in σ (step 6). If the correction is applied immediately, we can see that the pendant vertex u is removed from σ and that the value of v is flipped in σ. Edges on a branch in the forest will be added to κ until $v \in \sigma$, or a generator will be continuously moved from u to v until it encounters another generator, creating a correction path between two syndrome pairs.

Lemma 3.1 *A forest F is an undirected graph in which any two vertices are connected by at most one path. A forest F_G of some graph G is one in which some edges is removed such that there are no cycles in the graph, which satisfies the forest requirement.*
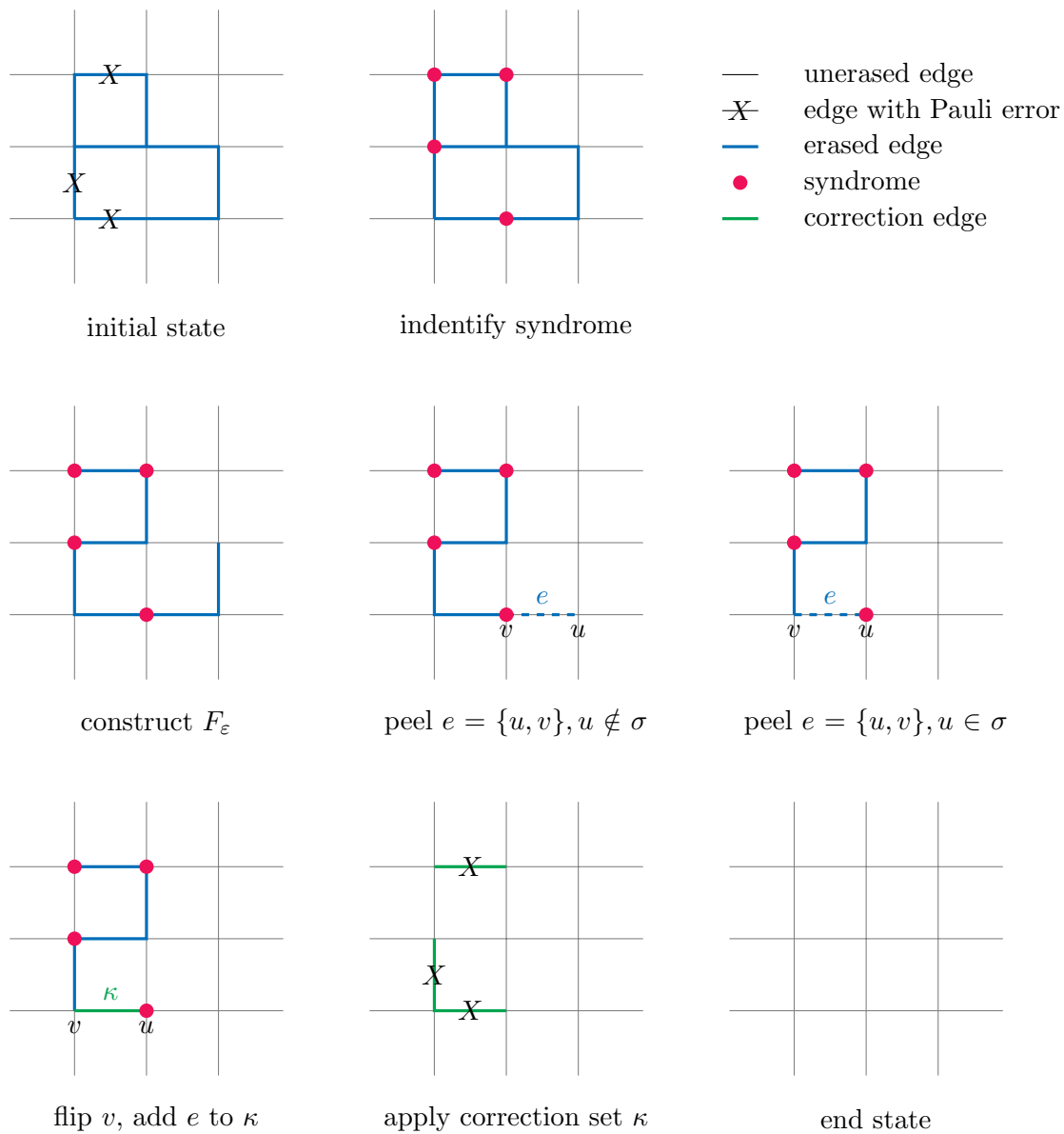
Figure 3.8: Schematic representation of the Peeling decoder.

Algorithm 1: Peeling decoder [8]

Data: A graph $G = (V, E)$, an erasure $\varepsilon \subset E$ and syndrome $\sigma \subset V$
Result: Correction set $\kappa \subset E$

1 construct a spanning forest F_ε of ε
2 initialize κ by $\kappa = \emptyset$
3 **while** $F_\varepsilon \neq \emptyset$ **do**
4   pick a leaf edge $e = u, v$ with pendant vertex u, remove e from F_ε
5   **if** $u \in \sigma$ **then**
6   add e to κ, remove u from σ and flip v in σ
7   **else:**
8   do nothing

9 **return** κ

Note that due the flipping of both u and v in σ, the parity of the number of generators in σ is always preserved. The peeling decoder can therefore always solve erasures with an even parity, as the size of σ will drop until at the end the syndrome will be empty $\sigma = \emptyset$, and call errors are corrected up to a stabilizer. This is always the case in the absence of measurement and Pauli errors, as all errors within the erasure either add or remove an even number of generators to or from σ.

Time complexity of the Peeling decoder   The spanning forest F_ε can be constructed in linear time. Also, the loop over the forest can be operated in linear if the list of leaves is pre-computed and updated during the loop. Thus the Peeling decoder has a linear time complexity in the size of the erasure $\mathcal{O}(|\varepsilon|)$ and therefore also in the number of qubits $\mathcal{O}(n)$.

Growing erasures

Now in the presence of Pauli errors, errors can occur on edges that are now not part of the erasure, and odd parity clusters can occur. Clusters that consists from only a single generator also exist, which are just end-points of syndromes caused by Pauli errors. We must therefore make an erasure ε from the syndrome σ that is compatible with the peeling decoder, which contains only even parity clusters. To do this, we can iteratively grow the clusters with an odd parity by an half-edge on the boundaries on the clusters. When two odd parity clusters meet, the merged cluster will have a even parity, and can now be solved by the peeling decoder.
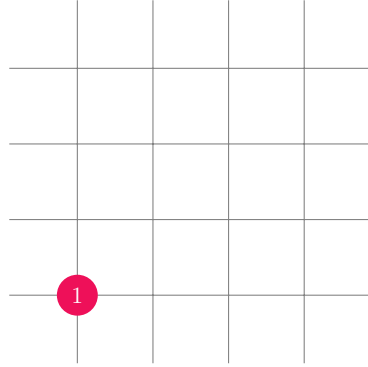
Union-Find algorithm

To keep track of the vertices of a cluster, it will be represented as a *cluster tree*, where an arbitrary vertex of the cluster will be the root, and any other vertex will be a child of the root. Whenever an edge (u, v) is fully grown, we will need to traverse the trees of the two vertices u and v, and check wether they have the same root; whether they belong to the same cluster. If not, a merge is initiated by making the root of smaller cluster a child of the bigger cluster. These functions, `find` and `union` respectively, are part of the Union-Find algorithm (not to be confused with the Union-Find decoder) [10].
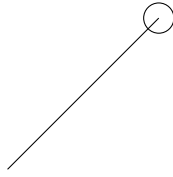
Within the Union-Find algorithm, two features ensure that the complexity of the algorithm is not quadratic. 1). With **path compression**, as we traverse a tree from child to parent until we reach the root, we make sure that each vertex encountered that we have encountered along the way is pointed directly to the root. This doubles the cost of the `find`, but speeds up any future call to any vertex on the traversed path. 2). With **weighted union**, we make sure to always make the smaller tree a child of the bigger tree. This ensures that the overall length of the path to the root stays minimal. In order to make this happen, we just need to store the size of the tree at the root.

Data structure   Now it is clear what information is exactly needed to grow the clusters using the Union-Find algorithm. We will need to store the cluster in a sort of cluster-tree. At the root of each tree we store the size and parity of that cluster in order to facilitate weighted union and to select the odd clusters. We will need to store the state of each edge (empty, half-grown, or fully grown) in a table called `support`. And we need to keep track of the boundary of each cluster in a `boundary` list.

The routine The full routine of the Union-Find decoder as originally described ([9], Algorithm 2) is listed in Algorithm 2. In line 1-2, we initialize the data structures, and a list of odd cluster roots $\mathcal{L}$. We will loop over this list until it is empty, or that there are no more odd clusters left.

In each growth iteration, we will need to keep track of which clusters have merged onto one, therefore the fusion list $\mathcal{F}$ is initialized in line 4. We loop over all the edges from the boundary of the clusters from $\mathcal{L}$ in line 5, and grow each edge by an half-edge in support. If an edge is fully grown, it is added to $\mathcal{F}$.

For each edge (u, v) in $\mathcal{F}$, we need to check whether the neighboring vertices belong to different clusters, and merge these clusters if they do. This is done using the Union-Find algorithm in line 6. We call find(u) and find(v) to find the cluster roots of the vertices. If they do not have the same root, we make one cluster the child of another by union(u,v). Note that this does not only merge two existing clusters, also new vertices, which have themselves as their roots, are added to the cluster this way. We also need to combine the boundary lists of the two clusters.

Finally, we need to update the elements in the cluster list $\mathcal{L}$. First, we replace each element u with its potential new cluster root find(u) in line 7. We can avoid creating duplicate elements by maintaining an extra look-up table that keeps track of the elements $\mathcal{L}$ at the beginning of each round of growth. In line 8, we update the boundary lists of all the clusters in $\mathcal{L}$, and in line 9, even clusters are removed from the list, preparing it for the next round of growth.

Algorithm 2: Union-Find decoder [9]

Data: A graph $G = (V, E)$, an erasure $\varepsilon \subset E$ and syndrome $\sigma \subset V$
Result: A grown erasure ε' such that each cluster $\gamma \subset \varepsilon$ is even

1. initialize cluster-trees, support and boundary lists for all clusters
2. initialize list of odd cluster roots $\mathcal{L}$
3. **while** $\mathcal{L} \neq \varnothing$ **do**
4.   initialize fusion list $\mathcal{F}$
5.   for all $u \in \mathcal{L}$, grow all edges in the boundary list of cluster C_u by a half-edge in support. If the edge is fully grow, add to fusion list $\mathcal{F}$
6.   for all $e = u, v \in \mathcal{F}$, if *find(u)* $\neq$ *find(v)*, then apply *union(u,v)*, append boundary list
7.   for all $u \in \mathcal{L}$, replace u with *find(u)* without creating duplicate elements
8.   for all $u \in \mathcal{L}$, update the boundary list
9.   remove even clusters from $\mathcal{L}$
10. run peeling decoder with grown erasure ε'

Time complexity of the Union-Find decoder

Chapter 4

Modifications to the Union-Find decoder

For the UF-decoder, each cluster C_α is represented by a set of vertices $\mathcal{V}_\alpha = \{v_1, v_2, v_3 ... v_{C_s^\alpha}\}$, where S_α is the size of the cluster. Here, the $\mathcal{V}_\alpha$ is stored in a tree, and each tree root is a unique identifier of the cluster. When new vertices v_{new} are added during $\texttt{Grow}(C_\alpha)$, they are added to the tree as a child of the root. When an edge is fully grown, we add it to a fusion list $\mathcal{F}$, and for all edges in $\mathcal{F}$ the vertex tree for the two neighboring vertices v_x, v_y are traversed to their roots using $\texttt{Find}(v_x)$ and $\texttt{Find}(v_y)$ respectively. If $\texttt{Find}(v_x) \neq \texttt{Find}(v_y)$ the cluster are merged using $\texttt{Union}(v_x, v_y)$ by making one vertex a child of another's root. The depth of the tree $\mathcal{V}^\alpha$ is kept low due to *path compression* and *weighted union* of clusters.

The vanilla UF-decoder (as described by Delfosse [9]) has an error threshold of 9.2% for a 2D toric lattice, that only suffers errors through a single Pauli channel. Delfosse has shown that the threshold can be improved by sorting the order of cluster growth, but has not provided a description of this sorting. In this chapter, we will show an implementation of this sorting routine that maintains a linear time complexity in section 4.2. In section 4.1, we will show an object oriented approach of the UF-decoder that allows for a straight forward data structure that is used for our implementation. In the remaining sections, we will show some other alterations to the UF-decoder, that uses the inspiration of the MLD-decoder or the MWPM-decoder to improve the error threshold while retaining a low time complexity.

4.1 Object oriented approach

Others who have implemented weighted growth (wrongly) use an algorithm that has a time complexity of $\mathcal{O}(n \log n)$, which is worse than the main algorithm [11]. We will introduce a weighted growth algorithm that has a linear time complexity, and therefore preserving the inverse Ackermann time complexity of the Union-Find decoder.

4.1.1 A new data structure

4.1.2 Finding clusters

4.2 Bucket Cluster Sort (BCS)

To further increase the error threshold for the Union-Find decoder from 9.2% to 9.9%, Delfosse implements *weighted growth*, where clusters are grown in increasing order based on their sizes [9]. However, the main problem with weighted growth is that the clusters now need to be sorted, and that after each growth iteration another round of sorting is necessary, due to the fact that the clusters have changed sizes due to growth and merges, and the order of clusters may have been changed. Nickerson has not given a description of how weighted growth is implemented. As the complexity of the algorithm is now dominated by the Union-Find algorithm, we need to make sure that weighted growth does not add to this complexity. To avoid this iterative sorting, we need to make sure that the insertion of a new element in our sorted list of clusters does not depend on the values in that list.

The Bucket Cluster sorting algorithm as described in this section is evolved from a more complicated version that is described in appendix A, which has a sub-linear complexity of $\mathcal{O}(\sqrt{n})$.

4.2.1 How to sort for weighted growth using BCS

Let us now first look at what weighted growth for the Union-Find decoder exactly does. When a cluster is odd, there exists at least one path of errors connecting this cluster to a generator outside of this cluster. When the cluster grows, a number of edges k that is proportional to the size S of the cluster is added to the cluster. If $k \propto S$ new edges are added, only $1/k$ of these edges will correctly connect the cluster with the generator. Therefore, more "incorrect" edges will be added during growth of a larger cluster.

Note however, that the benefit of growing a smaller cluster is not substantial if the clusters are of similar size. Take two clusters C_α, C_β with size $S_\alpha << S_\beta$, growth of cluster C_β will add $\sim k_\beta/2$ "incorrect" edges on average, whereas growth of cluster C_α will add $\sim k_\alpha/2 << k_\beta/2$ edges as $k_\alpha \propto S_\alpha$ and $k_\beta \propto S_\beta$. However, if $S_\alpha \simeq S_\beta$, the number of added "incorrect" edges for both clusters will also be similar, and it is the same when $S_\alpha = S_\beta$.

Lemma 4.1 *For two clusters C_α, C_β with size $S_\alpha << S_\beta$ the number of vertices in the clusters, $Grow(S_\beta)$ will add a smaller amount of* incorrect *edges to the cluster, which are edges that are not part of the matching.*

The sorting method that is suited for our case is *Bucket sort*. In this algorithm, the elements are distributed into k buckets, after which each bucket is sorted individually and the buckets are concatenated to return the sorted elements. Applied to the clusters, we sort the odd-parity clusters into k buckets, which replaces the odd cluster list $\mathcal{L}$. As the sizes of the clusters can only take on integer values, each bucket can be assigned a clusters size, and sorting of each individual bucket is not necessary. Furthermore, as we are not interested in the overall order of clusters, concatenating of the buckets is not necessary.

Growing a bucket

The procedure for the Union-Find decoder using the bucket sort algorithm is now to sequentially grow the clusters from a bucket starting from bucket 0, which contain the smallest single-generator clusters of size 1. After a round of growth, in the case of no merge event, these clusters are grown half edges, but are still size 1. We would therefore need twice as many buckets to differentiate between clusters without and with half-edges. Let us call them full-edged and half-edged clusters, respectively. Starting from bucket 0, even buckets contain full-edged clusters and odd buckets contain half-edged clusters of the same size. To grow a bucket, clusters are popped from the bucket, grown on the boundary, after which the clusters is to be distributed in a bucket again in a subroutine named `Place`.

$$\texttt{Place}(C) = \begin{cases} C \to b_{2(S_C-1)}, & \text{if } S_C \text{ even} \\ C \to b_{2(S_C-1)+1}, & \text{otherwise} \end{cases} \tag{4.1}$$

In the case of no merge event, clusters grown from even bucket b_i must be placed in odd bucket b_{i+1}, as it does not increase in size, and clusters grown from odd bucket j must be placed in even bucket b_{j+2k+1} with $k \in \mathbb{N}_0$ the number of added vertices. Also in the case of a union event of clusters C_α and C_β, the new cluster $\texttt{union}(C_\alpha, C_\beta) = C_{\alpha\beta}$ must be placed in a bucket $b_{\alpha\beta} > b_\alpha, b_{\alpha\beta} > b_\beta$. Thus we can grow the buckets sequentially, and need not to worry about bucket that have been already "emptied". This ensures that for two clusters C_α and C_β with $S_\alpha < S_\beta$, cluster A will be grown first, adding a fewer amount of "incorrect" edges as per lemma 4.1. Clusters of the same size $S_\alpha = S_\beta$ are placed in the same bucket and their order of growth is dependent on their order of placements.

All clusters within the same bucket are grown "together"; we first grow all the boundary edges of the clusters in the bucket by half, adding all fully grown edges to the fusion list $\mathcal{F}$ and check for the union and new boundary edges for all clusters together per algorithm 2. The order of growth within the bucket is dependent on the order of cluster placement into the bucket.

Theorem 4.1 *Weighted growth is achieved by growing the odd clusters sequentially starting from bucket b_0. Grown odd clusters from bucket b_c are added back to the bucket list using the `Place` subroutine, in a bucket b_g where $g > c$. Clusters C_α and C_β with $S_\alpha = S_\beta$ are placed int the same bucket b_{S_α}, and are grown together. However, their growing order is dependent on the order of placement within the bucket.*

Faulty entries

Now let us be clear: *only odd parity clusters will be placed in buckets, but each bucket does not only contain odd parity clusters.* As a merge happens between two odd parity clusters C_α and C_β during growth of C_β, cluster C_α has already been placed in a bucket, as it was still odd after its growth. But cluster C_α is now part of cluster AB and has even parity, and the entry of cluster C_α is faulty. To prevent growth of the *faulty entry*, we can check for the parity of the root cluster.
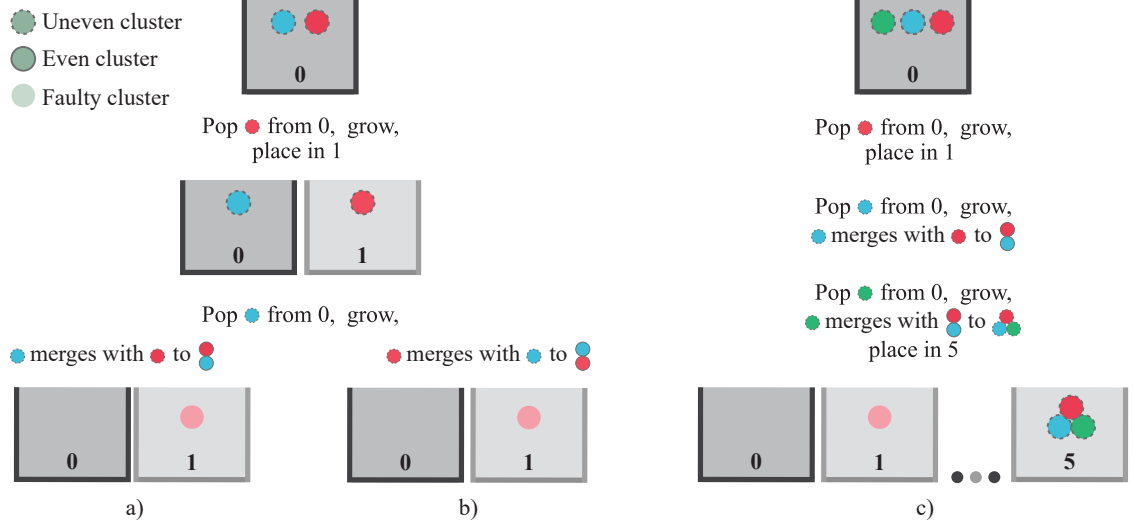
Figure 4.1: Faulty entries of clusters can occur in the buckets, a) cluster that should not be there due to a merge event. Situation a can be solved by checking the parity of the cluster. Checking the parity of the root cluster solves a) and b). Checking the bucket_number of the root cluster solves all.

Furthermore, it is possible that another cluster C_γ merges onto $C_{\alpha\beta}$, such that the cluster $C_{\alpha\beta\gamma}$ is odd again. Now, the faulty entry of cluster A passes the previous test. To solve this issue, we store an extra bucket number C_b at the root of a cluster. Whenever a cluster increases in size or merges to an odd parity cluster, we first update the C_b to the appropriate value and place it in its bucket. If the cluster merges to an even parity cluster, we update the C_b to *Null*. Now, every time a cluster is popped from bucket i, we can just check weather the current bucket corresponds to the C_b of the root cluster.

Lemma 4.2 *Each bucket b_i does not necessary contain clusters that still belong to b_i. Growth of these faulty entries are prevented by storing the bucket number j at the cluster $C_b = j$ during* `Place` *and checking for $i = j$ and odd cluster parity add the beginning of* `Grow`.

Number of buckets

How many buckets do we exactly need? On a lattice there can be n vertices, and a clusters can therefore grow to size n, spanning the entire lattice. Naturally, if a cluster spans the entire lattice, the solution given by the peeling decoder is now trivial. But we need to make sure that the decoder *can* give a solution. Consider an odd cluster C_μ of size S_α $n/2$ which covers half the lattice. There must exists another odd cluster C_β for matchings to exists, which has size $S_\beta \leq n/2$. As per lemma 4.1, C_β will grow before C_α. As the remaining

number of vertices is $n - S_\alpha - S_\beta$, C_β can never grow larger than C_α and will merge into C_α if no other odd cluster exists. There exists a maximum cluster size S_μ for which after $\texttt{Grow}(C_\mu)$ this is true. This cluster size S_μ is dependent on the code and the parity of lattice size L. We illustrate in figure 4.2 the clusters C_μ for the toric and planar code. Their maximum odd cluster size S_μ is listed in table 4.1, where $L' = L - 1$ for the planar code.

Lemma 4.3 *Once an odd cluster C_α has reached a size $S_\alpha > S_\mu$, it is certain that a smaller cluster C_β will grow in size before the bucket of C_α is reached, and it will merge into an even cluster $\texttt{Union}(C_\alpha, C_\beta) = C_{\alpha\beta}$.*

	L even	L odd
Toric	$S_\mu = L \times (\frac{L}{2} - 1) - 1$	$S_\mu = L \times (\frac{L'}{2} - 2) + (\frac{L'}{2} - 1)$
Planar	$S_\mu = L \times (\frac{L}{2} - 1)$	$S_\mu = L' \times \frac{L'}{2} - 1$

Table 4.1: The maximum cluster size S_μ for which it is not certain that another cluster will merge onto the current cluster, or the maximum cluster size for which a cluster is allowed to grow.

This maximum cluster size S_μ for growth determines the number of buckets $k + 1$ we will need.

$$k = 2(S_\mu - 1) \tag{4.2}$$

Any cluster with size $S \leq S_\mu$ will be placed into a bucket according to equation 4.1. If $S > S_\mu$, the cluster will not be placed into a bucket, and shall be assigned bucket number $C_b = Null$, as there is no bucket available.

Largest bucket occurrence

Not all buckets will be filled depending on the configuration of the lattice. It would therefore be redundant to go through all buckets just to find out that the majority of them is empty. To combat this, we can keep track of the largest filled bucket b_M. Whenever a bucket b_i has been emptied and $i = M$, we can break out of the bucket loop to skip the remainder of the buckets.

4.2.2 Complexity of BCS

Let us focus on the operations on a single cluster before it is grown an half-edge. A cluster is placed in a bucket, popped from that bucket some time after, checked for faulty entry, and if passed grown. All these operations are done linear time $\mathcal{O}(1)$. There are a maximum of $\mathcal{O}(L^2) = \mathcal{O}(N)$ buckets to go through. Thus the overall complexity of $\mathcal{O}(N\alpha(N))$ is preserved.

4.2.3 The BCS Union-Find decoder
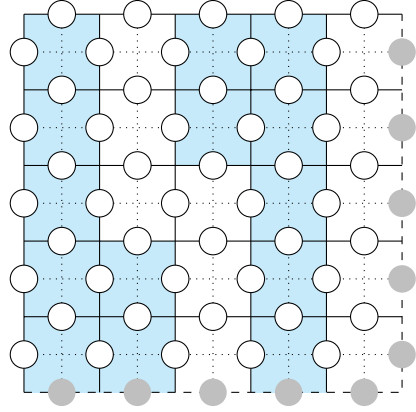
(a) Toric odd L = 5
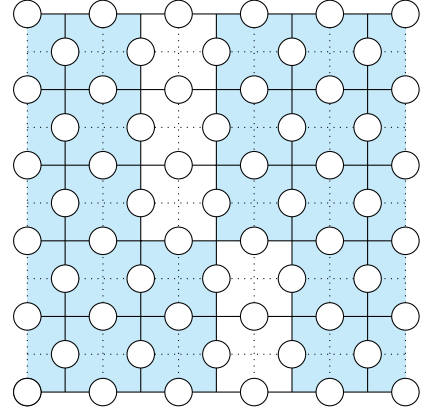
(b) Planar even L = 6
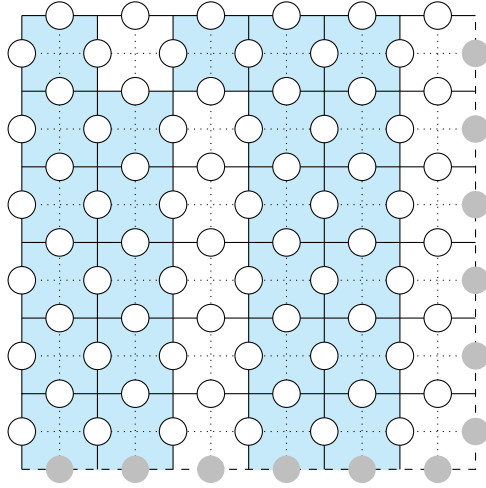
(c) Toric even L = 6
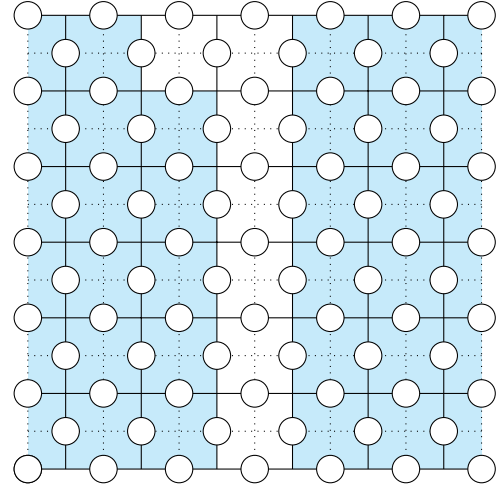
(d) Planar odd L = 7

Figure 4.2: The clusters C_μ with maximum cluster size S_μ that is allowed to grow is pictured for each case on the left. On the right, another cluster C_β is pictured that has a maximum size while still separated from C_μ.

4.3   Delayed Merge of boundary lists (DM)

When two clusters merge, one needs to check for the larger cluster between the two, and make the smaller cluster the child of the bigger cluster, which lowers the depth of the tree and is called the *weighted union rule.* Applied to the toric lattice, the Union-Find decoder also needs to append the boundary list (which contains all the boundary edges of a cluster) of the smaller cluster onto the list of the larger cluster. This method, as explained before, requires that the new boundary list needs to be checked again.

In our application, instead of appending the entire boundary list, we just add a pointer stored at the parent cluster to the child cluster. As a parent can have many children, the pointers are appended to a list `children`. When growing a cluster, we first check if this cluster has any child clusters. If yes, these child clusters will be grown first by popping them from the list, but any new vertices will always be added to the parent cluster. Also during and after a merge, we make sure that any new vertices are always added to the parent cluster. Any child will exist in the list of a parent for one round of growth, after which its boundaries will be grown, and the child is absorbed into the parent. This method also works recursively by keeping track of the root cluster instead of just the parent cluster, and many levels of parent-child relationships can exists, but again, only for one round of growth.
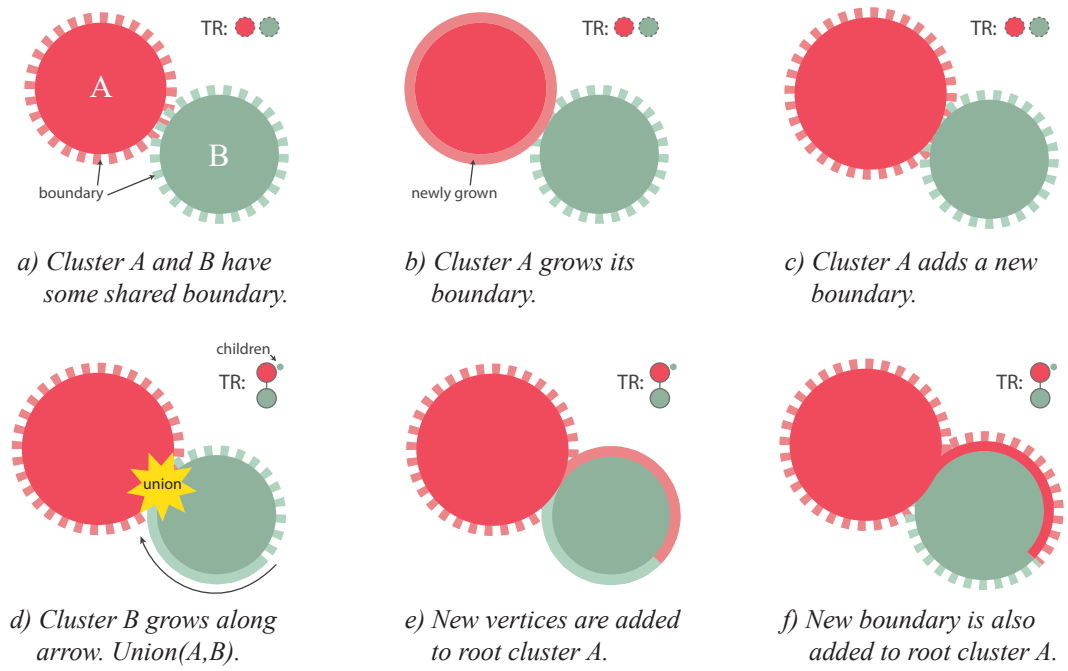
Figure 4.3: The parent-child method for merging boundary lists. By storing a list of pointers of child clusters at the parent cluster, we needn't append the full boundary list from the child to the parent cluster. The tree representation (TR) is shown on the top right.
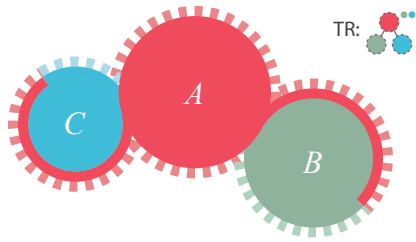
a) Cluster ABC with root cluster A is odd. Boundary of ABC is stored at root A, but also at children B and C.
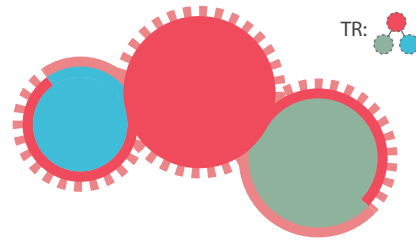
b) If cluster ABC grows, first the children are popped from the list and grown. New vertices are added to root A.
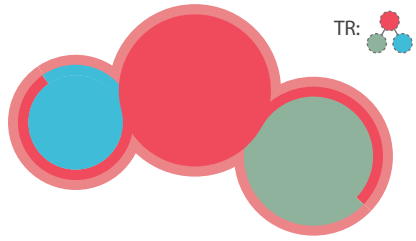
c) The boundary stored at root A is grow after.
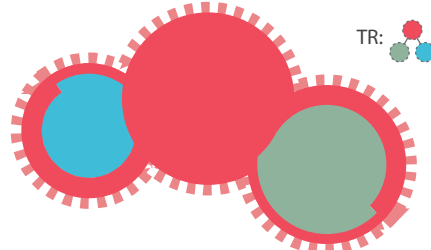
d) After growth, the children list is empty, and new boundary is stored at root A.

Figure 4.4: Growing a merged boundary using the parent-child method. The tree representation (TR) is shown on the top right.

4.4 Growing Edge Priority based on path degeneracy (GEP)

4.4.1 Degeneracy on connecting edges between Clusters (GEP-C)

4.4.2 Degeneracy on Vertices with connecting edges (GEP-V)

4.5 Balanced Bloom of cluster growth

Not all clusters should be grown at the same time. When grown, larger clusters relatively add more "incorrect edges" to themselves than compared to a smaller cluster (lemma 4.1). The UF-decoder therefore applies *weighted growth* of clusters, where the order of cluster growth is sorted based on the cluster sizes. We have shown a linear time implementation in the Bucket Cluster Sort in section 4.2. With the addition of weighted growth, the error threshold of the UF-decoder is increased from 9.2% to 9.9% for a 2D toric lattice [9]. This approaches but still lacks in terms of the 10.3% error threshold of the MWPM-decoder.

The UF-decoder is in fact a heuristic for minimum-weight matching. A large cluster is generally the result of multiple growth iterations of a given cluster. Each round of cluster growth buries the syndromes within that cluster with a layer of edges, of which a single edge or more will be part of the matching, and thus adds to the matching weight. With weighted growth, smaller clusters are grown first, such that this effect is less dominant. But the UF-decoder is unsurprisingly less successful at minimum-weight than the MWPM-decoder, which does this perfectly. The MWPM-decoder considers all possible matchings by constructing a fully connected graph where the edges have the distance between syndrome as weights. The UF-decoder does not look at the lattice in such a global way, but performs locally on each cluster. This should yield the same result conceptually, but it does not due to a major weakness; In each round of growth, all boundary edges are grown simultaneously, and the multiple potential merges is only handled after each round, where the order of the union operations is arbitrary. This leaves us with the question: Should all boundary edges of a cluster be grown simultaneously?

We suspect that the error threshold of the UF-decoder can be increased by improving the heuristic for minimum-weight matchings. In this section, we will accomplish this by sorting the order of boundary edge growth within a cluster by calculation of their potential matching weight. To keep a relatively low time complexity, we group the boundary edges by their root nodes, where the boundary edges in each node have the same matching weight. The calculation of the growth order, or growth delay in each node is done by traversal of the *node tree* of the cluster.

4.5.1 Potential matching weight

To show that not all boundary edges within a cluster should not be grown simultaneously, let us first consider an example. Cluster C_e consists of 3 vertices v_1, v_2, v_3 that lie on a horizontal line, distance 1 from each other, where each vertex has grown a half-edge an iteration before. Assume that each vertex in C_e is a syndrome; it therefore has odd

parity and is selected for growth. As UF-decoder performs on the cluster locally, it has no knowledge about its surroundings until it actually grows its edges.

Imagine some other cluster C_o with parity 1 and some size $S_o > 3$ lies adjacent to cluster C_e, where the growth of C_e will connect both clusters. The connecting edge e can either be touching vertex $v_e = v_1, v_2$ or v_3. The resulting matching will be between v_e and the syndrome vertex v_o in C_o on edges e and some edges of length l within C_o, and between edges $v_i \neq v_e$ in C_e. If $v_e = v_1$, the matchings will be $(v_1, v_o), (v_2, v_3)$ of weight $2+l$. Similarly for $v_e = v_3$, the matchings will be $(v_3, v_o), (v_1, v_2)$ of weight $2+l$. However if $v_e = v2$, the matchings will be $(v_2, v_o), (v_1, v_3)$, where the matching of v_1, v_3 has to traverse 2 edges, and has a total weight $3 + l$.

Let us call this calculation the *potential matching weight* (PMW) of some vertex $PMW(v_i)$, and leave out l as it is equal for all vertices. From the above example, we can see that even for a minimal sized odd cluster, the PMW is not equal for all vertices. It is not "fair" to grow all boundary edges simultaneously as the boundary edges connected to v_2 would add $+1$ to the matching weight. To grow fairly, the growth if these edges should be delayed for some iterations, which we will explore in section 4.5.3. But if the PMW is to be calculated for every vertex that has boundary edges for each cluster in each growth iteration, the time complexity of the algorithm would increase dramatically. Luckily, we can reduce these calculations to be performed on a set of *nodes* in each cluster.

Lemma 4.4 *The Potential Matching Weight (PMW) of a vertex v is the total length of matching edges within the cluster C_{grow} if the parity of the cluster C is even in an union between C_{grow} and C_{other}, where C_{other} is connected to C_{grow} on an edge touching v.*

4.5.2   Node representation of cluster

In the case of only Pauli errors, after syndrome identification, all identified clusters consist of a single vertex v_i which is also a syndrome σ_i. Let us call this original set of cluster $\mathcal{C}_0$. Within syndrome validation, these clusters are subjected to growth and merge events with other clusters. During growth, all vertices that are added to some cluster C have a closest syndrome σ within C that is in the original set of single-vertex/single-syndrome clusters $\mathcal{C}_0$. We say that these vertices are *seeded* in σ.

Let us call these seeds the *nodes n_i* of the cluster. From our previous example, each vertex in C_e is a syndrome in the original set $\mathcal{C}_0$, and therefore a node. In the example, we had calculated the PMW for each vertex. It turns out that the PMW is equal for all vertices with boundary vertices seeded in the same node. It is therefore sufficient to calculate the PMW for the nodes in the cluster.

Consider again the cluster C_e, where a merge event may not happen for many growth iterations. The number of vertices in C_e increases in each round of growth. However, the number of nodes remains the same at 3 nodes. Furthermore, we need only to calculate the PMW for the nodes in the cluster only once. We grow only the nodes with the smallest PMW in the cluster, and we can delay the growth of nodes with larger PMW. We can replace PMW by the *delay* in each node, the number of growth iterations to wait.

Balanced Bloom

We call the growth of the cluster in the subset of boundary edges that is seeded in n_i the *bloom* of node n_i. The flower of n_i is the subset of all vertices in the cluster seeded in the node. The size of the flower $n_i.s$ is the number of growth iterations a node has grown, and is equal to the maximum weight of edges grown from this node. The combined bloom of all nodes in a cluster is equivalent to the growth of the full cluster, where some nodes are to wait for some iterations based on their delay $n_i.d$.

The set of nodes $\mathcal{N} = \{n_1, n_2, ...n_{S_\mathcal{N}}\}$ is stored as a tree, an connected and acyclic graph, where the edges ϵ between the nodes are the branches in our figurative flower bush. Each node-edge ϵ can have arbitrary length and consists of one or more vertex-edges e. For any node set $\mathcal{N}$, we would like to difference in $n.d$ for all nodes in the set to be minimal. If the delays in the set is equal, we say that the set has reached *equal PMW*, as all boundary edges will lead to the same matching weight within the cluster. Once equal PMW is reached, the growth of a node set is the *balanced bloom* of nodes.

Lemma 4.5 *Every vertex v that is added to a cluster is seeded in some node n. All vertices with boundary edges that are seeded in the same node have the same delay $n.d$, the number of iterations to wait to reach a homogenous PMW in the cluster. A cluster, now defined by a node set $\mathcal{N}$, can be selectively grown by the bloom of a node $n \in \mathcal{N}$, growing the subset of boundary edges touching vertices seeded in n, where each node may have to wait for some iterations based on its delay, and the size of each node is stored as $n.s$, the number iterations it has grown.*

Junction-nodes

There is still one thing missing from this node representation of clusters. Consider our example cluster C_e of 3 nodes n_1, n_2, n_3 again. Now we slightly alter this cluster to C_e' by increasing the distance between n_1, n_2 and n_2, n_3 to two edges. This means that cluster C_e' is only established after two growth iterations of the three previous separate cluster of nodes n_1, n_2, n_3 and has a total size of 13 vertices. Now consider the vertices v_{12} and v_{23} that lie between n_1, n_2 and n_2, n_3, respectively. These are *merging vertices* as they are added to the cluster during an union of two merging clusters. It is not clear in which nodes these vertices are seeded, as they lie in equal distance to two nodes.

To solve this, we make these kind of vertices nodes of themselves, and call them *junction nodes* j. All nodes j have the same characteristics of syndrome nodes σ, and have their own delay and boundary edges seeded in them. The union of the set of junction nodes $\mathcal{J}$ and set of syndrome nodes (syndromes) $\mathcal{S}$ is equal to the node set $\mathcal{N}$.

Lemma 4.6 *On a merging vertex v that lie in equal distance to two syndrome nodes from two cluster merging into one, we initiate a junction node j in the node set $\mathcal{N}$. A junction node has the same properties as a syndrome node.*
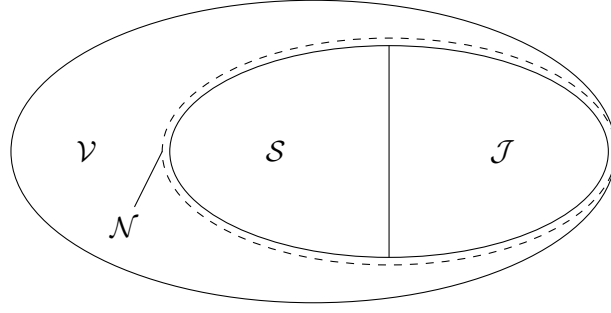
Figure 4.5: Sets

To sum up, all syndromes σ_i are nodes n_i, but not all nodes are syndromes. Furthermore, all nodes are vertices, but not all vertices are nodes. The node set size $S_{\mathcal{N}}$ is different from cluster size, which is the size of vertex set $\mathcal{V}$, and is referred to as $S_{\mathcal{V}}$ from now on. For any cluster C with vertex set $\mathcal{V}$ and node set $\mathcal{N}$, it is trivial that the node set size is upper bounded by the vertex set size, as all nodes are vertices, but not all vertices are nodes.

$$
\begin{aligned}
\mathcal{N} \subseteq \mathcal{V} \quad &, \quad S_{\mathcal{N}} \leq S_{\mathcal{V}} \\
\mathcal{S} \;\cup\; \mathcal{J} &= \mathcal{N} \\
\mathcal{S} \;\cap\; \mathcal{J} &= \varnothing
\end{aligned}
\tag{4.3}
$$

To be able to bloom each node separately, we cannot store the boundary edges of a cluster in a single list $\mathcal{L}$ at the cluster. Instead, we store the boundary list for each node n_i separately in their own boundary lists $n_i.\mathcal{L}$. Here we use the *object.property* notation to indicate that the property is stored at the parent object. As we will see in the next section, the calculation of node-delays is dependant on the direction in which $\mathcal{N}_\alpha$ is traversed. We store the node set by its root n_r at C_α.

Theorem 4.2 *The set of nodes $\mathcal{N} = \{n_1, n_2, ...n_{\mathcal{N}}\}$ of cluster C is a connected acyclic graph with root n_r, and exists next to the exists set of vertices $\mathcal{V}_\alpha$. The function of $\mathcal{N}_\alpha$ is to store the list of boundary edges at the nodes and growing each node according to the calculated node delay.*

4.5.3   Node parity and delay

The calculation of the PMW for each node in a cluster is a heavy task, as for each node the entire clusters needs to be checked on which edges are part of the matching and results to a quadratic complexity. Luckily, the complexity can be reduced to linear by the calculation of the relative *delay* of each node, where the tree of the node set is traversed.

41

1D node tree

To show how this calculation is performed, we first take the example of a 1D node tree $\mathcal{N}_{1D}$ of size $S_\mathcal{N}$, where all nodes lie on one line, but are allowed to grow in x and y directions. In our example, we only look at the first 3 nodes n_1, n_2, connected by edge ϵ_1, and n_3, connected to n_2 by edge ϵ_2. The node tree continues after n_3 for $S_\mathcal{N} - 3$ nodes. Note that edges of the node set are indicated by ϵ, whereas edges of the vertex set are indicated by e.

Recall that the size of the node $n.s$ is equal to the iterations it has grown, one half-edge per iteration. This means that if a merge with some other cluster occurs on a boundary edge of n, the weight of the matchings edges within the flower of n is equal to $\lfloor n.s/2 \rfloor + 1$ or. For a merge on n_1, we also add edge ϵ_2 and some value k corresponding to the weight of matchings in the remainder of the cluster. Let us calculate the PMW values for each of nodes n_1, n_2, n_3.

$$
\begin{aligned}
PMW(n_1) &= \lfloor n_1.s/2 \rfloor + 1 + \epsilon_2 + k \\
PMW(n_2) &= \lfloor n_2.s/2 \rfloor + 1 + \epsilon_1 + \epsilon_2 + k \\
PMW(n_3) &= \lfloor n_3.s/2 \rfloor + 1 + \epsilon_1 + k
\end{aligned}
$$

By taking the summed difference in PMW values in subsequent nodes, the relative delay of a node $n.d$ can be calculated with respect to the first node. In this differential, we set $n_1.d$ of the first node to zero.

$$
\begin{aligned}
n_1.d &= 0 \\
n_2.d &= PMW(n_2) - PMW(n_1) + n_1.d = 2(\lfloor n_2.s/2 \rfloor - \lfloor n_1.s/2 \rfloor + \epsilon_1) + n_1.d \\
n_3.d &= PMW(n_3) - PMW(n_2) + n_2.d = 2(\lfloor n_3.s/2 \rfloor - \lfloor n_2.s/2 \rfloor - \epsilon_2) + n_2.d
\end{aligned}
$$

These delay values are not entirely correct, as $n_1.s = n_2.s = 2i$ yields the same value as $n_1.s = 2_i, n_2.s = 2)i + 1$. We introduce growth support of a node $n.g = n.s \bmod 2$ to accommodate for this degeneracy in PMW, and add this to the delay values.

$$
\begin{aligned}
n_1.d &= 0 \\
n_2.d &= 2\big(\lfloor (n_2.s + n_2.g)/2 \rfloor - \lfloor (n_1.s + n_2.g)/2 \rfloor + \epsilon_1\big) - (n_1.g + n_2.g) \bmod 2 + n_1.d \\
n_3.d &= 2\big(\lfloor (n_3.s + n_3.g)/2 \rfloor - \lfloor (n_2.s + n_3.g)/2 \rfloor - \epsilon_2\big) - (n_3.g + n_2.g) \bmod 2 + n_2.d
\end{aligned}
$$

If we were to consider some nodes $n_4, n_5...$ as well, we would find a trend in which the delay calculation is dependant on the *parity* of the node number i. The delay of odd node n_{2i+1} has the positive addition of ϵ_{2i+1} in its delay value, and the substraction of ϵ_{2i} for an even node n_{2i}. Thus we can generalize the delay calculation as the following:

$$
n_i.d = n_{i-1}.d + 2\left(\left\lfloor \frac{(n_i.s + n_i.g)}{2} \right\rfloor - \left\lfloor \frac{(n_{i-1}.s + n_i.g)}{2} \right\rfloor + (-1)^{i+1}\epsilon_{i-1} \right)
$$
$$
- (n_i.g + n_{i-1}.g) \bmod 2 \quad | \quad n_0.d = 0. \quad (4.4)
$$

Using equation 4.4, we can calculate all the relative delays in the 1D tree by traversing the node tree just once from left to right. The initial delay $n_0.d$ can be set at any arbitrary value, as there may be some odd node n_i in the tree that has $n_i.d < n_0.d$. For each node set, we therefore need to store the *minimal delay value*. This value can be stored at the cluster object $C.d$. To grow a cluster, we first calculate its node delays. Then, in each round of growth, we traverse the node tree to find nodes where $n.w = n.d - C.d$, where $n.w$ is the number of growth iterations a node has *waited*. For all nodes that do not satisfy, we add 1 to its waited value.

Node tree parity

The 1D node tree does not accurately represent node trees that occur on a real lattice. On a 2D (Pauli errors) and 3D lattice (Pauli and measurement errors), the node tree is allowed to form in the same dimensions. But as $\mathcal{N}$ is an acyclic graph, the 3D variant can be considered equal to the 2D variant. The difference is that now the *ancestry* in the tree, the set of parent-child relations, is not determined by some number i, and each node can have more than 2 connections.

The delay calculation is done comparatively with the previous node, which means that there must be some directed path within $\mathcal{N}$, such that there is a clear direction to traverse the tree for the delay calculation. We can start the calculation from the root n_r. The node parity, previously determined by the number i, is now set by the number of children nodes modulo 2. To calculate this parity for each node without traversing all children nodes, we can use the following function

$$n_\beta.p = \begin{cases} 0, & \text{if } n_\beta \text{ has no children} \\ (\sum_j 1 - n_{\gamma,j}.p) \bmod 2 \mid \forall n_\gamma \text{ child of } n_\beta, & \text{otherwise,} \end{cases} \qquad (4.5)$$

where n_β is the node of interest, and each of the nodes $n_{\gamma,j}$ is a child of n_β. As this requires the parity of each child node to be known, the node parities of the entire set can be calculated by a depth-first search (DFS) of the node tree, and traversing back to the root recursively and applying the above equation.

Since $\mathcal{N}$ is acyclic, any node in the set can be set as the root n_r of the set, and the calculation of the parity would still be valid, although not identical. The node set $\mathcal{N}$ is therefore a *semi*-directed tree, in which the edges are undirected, but an ancestry is set by the root node n_r. If the root node changes to n_r', the ancestry within the tree changes, and the node parities within the set become unknown, or *undefined*, requiring a new calculation of a reversed DFS from n_r'.

Lemma 4.7 *Any node $n_i \in \mathcal{N}_\alpha$ is a valid root.*

Lemma 4.8 *The node parity $n_i.p$ is defined as of the number of children nodes of node n_i modulo 2, and can be calculated via a reversed DFS from root n_r. If a new node is set as root n_r', the ancestry in a set changes, rendering node parities within the set to "undefined".*

Node tree delay

The delay equation 4.4 can be altered by replacing the node number i with some parent-child relationship between nodes, similarly to the parity calculation. To calculate the node delays within $\mathcal{N}$, we need to traverse $\mathcal{N}$ in a second DFS from root n_r with

$$
n_\beta.d = n_\alpha.d + 2\left(\left\lfloor \frac{(n_\beta.s + n_\beta.g)}{2} \right\rfloor - \left\lfloor \frac{(n_\alpha.s + n_\beta.g)}{2} \right\rfloor + (-1)^{n_\beta.p-1+1}\epsilon_\beta \right)
$$
$$
- (n_\beta.g + n_\alpha.g) \bmod 2 \quad | \quad n_r.d = 0, \ n_\beta \text{ child of } n_\alpha, \quad (4.6)
$$

where n_β is the node of interest and n_α is an ancestor of n_β, and the sign of the edge component is now dependant on the node parity $n.p$. As the node parities are only defined while the same node is root per lemma 4.8, the delay calculation is only valid if the DFS is performed from the same root n_r as in the parity calculation.

Lemma 4.9 *The calculation of node delays is only valid while node parities within the set are defined along the same ancestry as the node delay calculation.*

An interesting aspect of the node delays is that the relative differences in delays in neighboring nodes are the some for any node as root $n_r = n \forall n \in \mathcal{N}$. The actual delay value may differ for different roots as we always set $n_r.d = 0$. This is the reason that when blooming a node, we check for $n.w = n.d - C.d$, as $n.d - C.d$ for each node is the same for any node as root. This fact strengthens lemma 4.7.

Junction node parity and delay

Up until now, we have neglected junction-nodes in our story on node parity and delays. But as junction nodes have the same properties as syndrome nodes, there also exists edges seeded in junction nodes, and thus they must be included in the parity and delay calculations. Furthermore, without junction nodes, lemma 4.7 cannot be true for a node set $\mathcal{N}$ for all nodes $n \in \mathcal{N}$ for the same set of edges $\{\epsilon\}$.

As a junction node is also allowed to bloom, similarly to a syndrome node, equation 4.6 still holds for junction nodes. However, the parity of a junction node is calculated differently. Consider an example node set $\mathcal{N}_e$ with 5 syndrome nodes $\{\sigma_1, ..., \sigma_5\}$ lined up linearly with distance 1 between them and $n_r = \sigma_1$. Let us drop the $n.s, n.g$ components of the delay in equation 4.6 as we are now only interested in the parity component $(-1)^{n_\beta.p-1+1}\epsilon_\beta$. The parity of σ_4 is odd, therefore

$$
\sigma_4.d = \sigma_3.d + 2(\sigma_3, \sigma_4),
$$

where $\epsilon = (\sigma_3, \sigma_4)$ is an edge connecting two nodes.

Consider now a second example node set $\mathcal{N}_e'$ with 3 syndrome nodes and 2 junction nodes $\{\sigma_1, j_2, \sigma_3, j_4, \sigma_5\}$. The PMW's for σ_3 and j_4 are $(\sigma_1, j_2) + (j_4, \sigma_5)$ and $(\sigma_1, j_2) + (\sigma_3, j_4) + (j_4, \sigma_5)$, respectively, where the delay in j_4 is now

$$
j_4.d = \sigma_3.d - 2(\sigma_3, j_4).
$$

44

We see that the edge component of the delay calculation now has an opposite sign. This flip in sign is due to a flip in node parity for junction nodes compared to syndrome nodes. As a result, we can generalize the parity calculation of equation 4.5 for realistic node sets.

$$n_\beta.p = \begin{cases} 0, & \text{if } n_\beta \text{ has no children} \\ \left(\sum_j 1 - n_{\gamma,j}.p \right) \bmod 2 \mid \forall n_\gamma \text{ child of } n_\beta, & n_\beta \equiv \sigma_\beta \\ 1 - \left(\sum_j 1 - n_{\gamma,j}.p \right) \bmod 2 \mid \forall n_\gamma \text{ child of } n_\beta, & n_\beta \equiv j_\beta \end{cases} \qquad (4.7)$$

To put this into perspective of lemma 4.8, the parity of a syndrome node is the number of children *syndrome* nodes. The parity of a junction node is 1 minus the number of children syndrome nodes. From here, our definition of parity and delay calculation stays unchanged; the parities can to be calculated by a reversed DFS of the node tree from the root with equation 4.7, and the delays by a second DFS with equation 4.6.

Lemma 4.10 *The node parity in a syndrome node $\sigma.p$ is the number of children syndrome nodes σ_γ modulo 2. The node parity in junction node $j.p$ is 1 minus the above definition.*

To perform a reverse DFS of the node tree, we can use a *head recursive* function that calls itself, where the recursiveness is before the required routine. The parity calculation is then the following algorithm.

Algorithm 3: CalcParity

Data: node
Result: Defined parities for all children of node

1   parity = Sum([1− CalcParity(child) $\forall$ child *of* node]) %2
2   **if** node $\equiv \sigma$ **then**
3 | node.p = parity
4   **elif** node $\equiv j$ **then**
5 | node.p = 1− parity
6   **return** node.p

Degree of delay due to parity inversion

With equation 4.6, we can calculate the appropriate delays in nodes such that if the bloom in these nodes are delayed for that many iterations, the PMW's for every node in the set is equal. We will see how to grow a node set in section 4.5.4. After that, we will see how to join two node sets in the case of a merge of two clusters in section 4.5.5. But before we move on, we already see a problem arising in the parity and delay calculations.

If some odd number of nodes $\mathcal{N}_o$ is attached to n^e of $\mathcal{N}_e$ during a join operation of two node sets, node parities for nodes in subset $\mathcal{N}'_e = \{n_i \in \mathcal{N}_e | n_i \text{ ancestor of } n^e\}$ are flipped, where odd nodes become even and even become odd, which is called *parity inversion*. Per lemma 4.9, the delays in $\mathcal{N}'_e$ are now undefined and need to be recalculated. If before the join operation, $\mathcal{N}_e$ had grown for some iterations where the odd nodes have waited

(approaching equal PMW), the even nodes will have some node sizes larger than the odd node sizes $n_{even}^e.s > n_{odd}^e.s$. After the join operations, the parities for nodes in $\mathcal{N}_e'$ flip, and now the previously-even odd nodes have some positive delay. As $n_{even}^e.s > n_{odd}^e.s$, these delays will increase in value per equation 4.6 compared to the previous delay calculation.

As the lattice increases in size, the number of merges between clusters or join operations between node sets will also increase. The node parities for some parts of some node sets will suffer parity inversion during these merges, leading to increasingly larger delay values. The delayed bloom of nodes may therefore not be balanced at all with the current delay equation. We therefore introduce a parameter $K_{bloom} \in [0,1]$ that determines the degree of delay of a node.

$$
\begin{aligned}
n_\beta.d = n_\alpha.d + \left\lceil K_{bloom}\left(2\left(\left\lfloor \frac{(n_\beta.s + n_\beta.g)}{2} \right\rfloor - \left\lfloor \frac{(n_\alpha.s + n_\beta.g)}{2} \right\rfloor + (-1)^{n_\beta.p-1+1}\epsilon_\beta\right)\right.\right. \\
\left.\left. - (n_\beta.g + n_\alpha.g) \bmod 2\right)\right\rceil \quad | \quad n_r.d = 0, \ n_\beta \text{ child of } n_\alpha, \quad (4.8)
\end{aligned}
$$

From intuition the degree of delay should be set to $K_{bloom} = 1/2$. For this value, the delays in a node set are halved, such that in the case of parity inversion, the delay values from before and after the inversion are kept at minimum. But as the inversion of parities mostly does not occur on all nodes in a set, this is not necessarily true, and other values of K_{bloom} should be explored.

Lemma 4.11 *The degree of delay K_{bloom} determines the part of the calculated delays that is actually assigned to the nodes. This is to minimize the node delays in new delay calculations in nodes that have suffered parity inversion after a join operation with another node set.*

The delay calculation is done by a DFS of the node tree, which can be done by a *tail recursive* function. Here the recursiveness is after the routine, which satisfies the DFS. The delay calculation is then the following algorithm.

Algorithm 4: CalcDelay

Data: node, cluster
Result: Defined parities for all children of node

1 **if** node *has an ancestor* **then**
2   calculate node.d with equation 4.8
3   **if** node.d < cluster.d **then**
4   cluster.d = node.d

5 **for** child *of* node:
6   CalcDelay(child, cluster)

Parity and delay routines

With equation 4.7 and 4.8, we now finally have the tools to formulate the algorithms to calculate the node parities and delays. For a node set with root n_r, we can calculate the parities by calling the head recursive function `CalcParity` on n_r in algorithm 3, where we do a reverse DFS of the node tree. The node delays are calculated by calling the tail recursive function `CalcDelay` in algorithm 4, where we do a second DFS of the node tree.

Theorem 4.3 *To prepare a cluster with node set $\mathcal{N}$ and node root n_r with undefined node parities and delays, we calculate node parities in $\mathcal{N}$ by calling the head recursive function* `CalcParity`(n_r)*, and sequentially calculate node delays in $\mathcal{N}$ by calling the tail recursive function* `CalcDelay`(n_r)*.*

4.5.4 Growing a cluster

The boundary list for each cluster is not stored at C, but separately stored at each of the nodes n_i in $\mathcal{N}$. To grow a cluster `Grow`(C), we now traverse all $n_i \in \mathcal{N}$ from the root n_r and apply `Bloom`(n_i), which increases the support of all boundary edges in $\mathcal{L}_{n_i}$ at node n_i by 1. If this node hasn't waited enough $n_i.w - n_i.d - C.d > 0$, we skip this node, add to the wait $n_i.w = n_i.w + 1$ and apply `Bloom` on its children. New vertices v_{new} grown from node n_i are added to $\mathcal{V}$, while storing the seed node at each new vertex $v_{new}.n = n_i$. New boundary edges are appended to the boundary list $n_i.\mathcal{L}$ stored each seed node n_i. The number of nodes in $\mathcal{N}$ and the shape of the flower bush tree therefore does not change while no merge between clusters has happened.

Theorem 4.4 *A cluster C is grown by calling* `Bloom`(n_r)*, which first checks for the wait of the current node $n_i.w - n_i.d - C.d > 0$ to grow its boundary edges, and then recursively applies* `Bloom` *to its children.*

4.5.5 Joint of node sets

With the addition of the node set $\mathcal{N}$, during a union of clusters C_α and C_β, we have to additionally combine the node sets $\mathcal{N}_\alpha$ and $\mathcal{N}_\beta$. Let us first make a clear distinction between the various routines. On the vertex set $\mathcal{V}$ we apply `Union`(v^α, v^β), on the two vertices spanning the edge connecting two clusters. On node set $\mathcal{N}$, we introduce here `Joint`(n^α, n^β), which is called on the two nodes n^α, n^β that seeds vertices v^α, v^β, respectively. From now on, when we talk about the "merge clusters C^α and C^{β}", "the union of vertex sets $\mathcal{V}_\alpha$ and $\mathcal{V}_\beta$" or the "joint of node sets $\mathcal{N}_\alpha$ and $\mathcal{N}_\beta$", we always refer to the combination of these two routines.

   Within the vertex set $\mathcal{V}$, we apply *path compression* and *weighted union* to minimize the depth of the tree and therefore minimizing the calls to the `Find` function. Similarly, in the node set $\mathcal{N}$, we would also like to apply a set of rules to minimize the calls to `CalcParity` and `CalcDelay`. As the structure of the tree is crucial in computing the parities and relative delays between the nodes, these rules will be quite different than in vertex set $\mathcal{V}$. First of

all, we note that while the node set does not change, the parities and delays within the node set stay valid.

Lemma 4.12 *While node set $\mathcal{N}$ is unchanged, the calculated parities and delays within the set are valid.*

Our rules will be dependant on the parities of the joining node sets, which is the number of syndrome-nodes in the set modulo 2. This is due to that junction-nodes do not add to the count of the number of children nodes per lemma 4.10. Note that the parity of a node set $\mathcal{N}.p$ is therefore exactly the same as the parity of a cluster $C.p$, which also refer to the number of syndromes in the cluster.

Lemma 4.13 *The parity of node set $\mathcal{N}.p$ is the number of syndrome-nodes $a_i \in \mathcal{N}$ modulo 2. The parity of node set $\mathcal{N}.p$ is analogous to cluster parity $C.p$.*

Joint to even node set

Let us first consider the joint operation of two or more node sets, where the resulting node set $\mathcal{N}_e$ is even. If we calculate the parities of a node set with even parity $\mathcal{N}_e$, we will end up with an odd node $n_r.p = 0$ as root of node set $\mathcal{N}_e$. It therefore does not make sense to talk about node parities within an even node set. Luckily, but not coincidentally, if a node set is even, the cluster is even and therefore will not grow. We could say that we need not to worry about the parties and delays within $\mathcal{N}_e$.

Lemma 4.14 *Node parities become undefined if multiple node sets joins into a new set $\mathcal{N}$ with even parity.*

However, it is entirely possible that another cluster grows, and merges onto the cluster of $\mathcal{N}_e$. In that case, we might think about recovering some of the node parities and delays that were calculated in the subsets of $\mathcal{N}_e$, such that we don't have to traverse $\mathcal{N}_e$ entirely for its parities and delays.

Joint to odd node set

Consider the joint operation of an even $\mathcal{N}^e$ and an odd node set $\mathcal{N}^o$ in nodes n^e, n^o respectively, and assume that this joining is due to the growth of odd cluster $\mathcal{N}^o$ onto an "idle" $\mathcal{N}^e$. The joint of these two sets leaves a new odd node set $\mathcal{N}^o_{new}$ with subsets $'\mathcal{N}^e$ and $'\mathcal{N}^o$, referring to the original node sets. We are provided with two choices, a) make n^e child of n^o, or b) make n^o child of n^e. Note that the child node n^c will become the *sub-root* in subset $'\mathcal{N}^c$, where the ancestry in the subset has been reset in the new sub-root, and is allowed per lemma 4.7.

If the subset $'\mathcal{N}^e$ consists of only two odd node sub-subsets $''\mathcal{N}^o_0, ''\mathcal{N}^o_1$, where n_0, n_1 are the joining nodes, the ancestry in $''\mathcal{N}^o_0$ is preserved and n_1 is the sub-root of $''\mathcal{N}^o_1$. We see

that the parities in all ancestors of n_0 are flipped. Let's consider the cases and find whether we can minimize the parity and delay calculation in $'\mathcal{N}^e$.

For case a), an even number of nodes of $'\mathcal{N}^e$ is attached to n^o, and the ancestry in $'\mathcal{N}^o$ hasn't changed. This means that the parities in $'\mathcal{N}^o$ do not change per lemma 4.8, and the delays in $'\mathcal{N}^o$ are still valid as per lemma 4.9. In $'\mathcal{N}^e$, as the ancestry path has changed, we are certain to traverse $'\mathcal{N}^e$ from the sub-root n^e to calculate the delays in this subset which is in the order of $S_{'\mathcal{N}^e}$.

In case b), as an odd number of nodes of $'\mathcal{N}^o$ is attached to n^e, it means that parities of all ancestor of n^e are flipped. As the ancestry in $'\mathcal{N}^o$ has changed, we are certain to traverse $'\mathcal{N}^o$ from the sub-root n^o to calculate the delays which is in the order of $S_{'\mathcal{N}^o}$. The node parity changes in $'\mathcal{N}^e$ will be dependant on the location of n^e in the ancestry compared to n^1 and n^2, and all children nodes of these parity changes will have to recalculate their delays. Let's call the number of nodes needs to calculate parity and delays in $'\mathcal{N}^e$ a value $S_e \leq S_{'\mathcal{N}^e}$, leaving the total number of operations in the order of $S_e + S_{'\mathcal{N}^o}$.

For $'\mathcal{N}^e$ consisting of two subsets, keeping track of the parity changes between n^e, n^0 and n^1 is still an easy task, and we might gain in minimization in operations in case b) compared to case a) for some value S_e such that $S_e + S_{'\mathcal{N}^o} < S_{'\mathcal{N}^e}$. But as the number of subsets in $'\mathcal{N}^e$ increases, the task of finding the ancestry paths of parity changes becomes analogous to traversing $'\mathcal{N}^e$ entirely $S_e \rightarrow S_{'\mathcal{N}^e}$. To simplify, we always choose case a.

Theorem 4.5 *The union of node sets $\mathcal{N}^\alpha, \mathcal{N}^\beta$ on nodes n^α, n^β respectively is performed with $\texttt{Joint}(n^\alpha, n^\beta)$. If the resulting node set $\mathcal{N}$ is odd, one of $\mathcal{N}^\alpha$ and $\mathcal{N}^\beta$ is odd while the other is even, and $\texttt{Joint}(n^\alpha, n^\beta)$ makes the node of the even set n^e a child of the node of the odd set n^o. If the resulting node set $\mathcal{N}$ is even, the choice is arbitrary.*

4.5.6 Multiple joints per bucket

Clusters with same vertex set size $S_\mathcal{V}$ lie in the same bucket b_i and thus are grown together per theorem 4.1. Let's call the growth of all clusters in a bucket a *growth iteration*. As the state of fully grown edges are only checked after each growth iteration including possibly many clusters, there may be multiple joint events within the same growth iteration. If the node parities and delays are to be calculated on all the union events in the fusion list $\mathcal{F}$, some node parity and delay calculations may be invalid and unnecessary.

Consider an example with 5 odd clusters $C_1, ... C_5$ with node sets $\mathcal{N}_1, ... \mathcal{N}_5$. The union of C_1 and C_2 to C_{12} is odd-odd and requires no parity-delay calculation. The union of C_{12} and C_3 is even-odd, and we calculate the parities and delays in the $\mathcal{N}_{12}$. The union of C_{123} and C_4 is odd-odd and the union of C_{1234} and C_5 is even odd, and we calculate the parities and delays in $\mathcal{N}_{1234}$. The earlier computation in $\mathcal{N}_{12}$ was therefore unnecessary and possible invalid.

To circumvent this even parity multiplicity, we must make sure to only apply the calculation to the largest even node set in some sequence of joint operations. To do this, we first note that some odd node set $\mathcal{N}^o$ must always consist of some odd part $'\mathcal{N}^o$ and

an even part $'\mathcal{N}^e$. The even part $'\mathcal{N}^e$ may be subdivided into a number of odd and even sub-subsets, as long as the sum is even.

Lemma 4.15 *An odd node set $\mathcal{N}$ that is the result of some joint operations must consist of an odd subset $'\mathcal{N}^o$ and an even subset $'\mathcal{N}^e$, where the even subset $'\mathcal{N}^e$ may consist of smaller sub-subsets $''\mathcal{N}$.*

This even subset $'\mathcal{N}^e$ is the undefined part of $\mathcal{N}^o$ in which we must calculate the parities and delays. As we can only be sure that the subset $'\mathcal{N}^e$ is complete after all unions of clusters are complete, we cannot apply and parity-delay calculations during the unions. We suspend these calculations as much as possible by doing them just before a cluster is grown from a bucket.

Lemma 4.16 *Parity and delay calculations are only performed on a the undefined part of a node set when a cluster is grown, not directly after a joint operation.*

The only task now is to store where the even subset $'\mathcal{N}^e$ starts in the ancestry of subset $\mathcal{N}^o$. For each joint operation between odd node set $'\mathcal{N}^o$ and even node set $'\mathcal{N}^e$ on nodes n^o, n^e per theorem 4.5, we store the sub-root $'n_r^e$ of subset $'\mathcal{N}^e$ to a list $\mathcal{C}$ at the root node of the resulting set $\mathcal{N}^{res}$ of cluster C^{res}. If cluster C is selected for growth as per theorem 4.1, we first check for nodes in $n^r.\mathcal{C}$ at root and apply `CalcParity`(n_i) and `CalcDelay`(n_i) for all nodes $n^i \in n^r.\mathcal{C}$ to calculate parities and delays in undefined parts of the set. We then call `Bloom`(n_r) per theorem 4.4.

Theorem 4.6 *Undefined parts of an odd node set $\mathcal{N}^o$ are defined as a set $\mathcal{C}_{\mathcal{N}^o}$ of sub-roots from which all children (including sub-roots) are undefined, and is stored at root node n_r^o. If before it has grown, node set $\mathcal{N}^o$ is joint with another odd node set, which then act as the even set $^\uparrow\mathcal{N}^e$ in a larger joint event, the sub-root of $^\uparrow\mathcal{N}^e$ is stored at $n_r^{\uparrow\mathcal{N}^o}$. Delay and parity calculations will then traverse all undefined paths only once.*

4.5.7 Pseudocode

4.5.8 Complexity of Balanced Bloom

The contribution to the time complexity of the UF-EG decoder compared to the UF-decoder can be divided into two parts. First is the contribution by `CalcParity` and `CalcDelay`. As these two functions are always called together per theorem 4.6, we can just introspect the number of calls to one of them, and call this contribution the *delay* complexity. The second contribution will be caused by `Grow`, as now we have to additionally traverse the node set tree's of each cluster to access its boundary edges and grow them with `Bloom` as compared to a single boundary list per cluster. We call this second contribution the *bloom* complexity.

Delay complexity

Consider an odd cluster represented by node set $^{k-1}\mathcal{N}^o$ with set size $S_{k-1}\mathcal{N}^o$ that is the result of union between a number of clusters ^kC_i with node subsets $^k\mathcal{N}_i$. Here k indicates a *generation*, where larger k indicates a more distant descendent generation of smaller clusters. As $^{k-1}\mathcal{N}^o$ is odd, it will be selected for growth. And because it consists of a number of subsets, $^{k01}\mathcal{N}^o$ is bound to consist of an odd subset $^k\mathcal{N}_0^o$ and an even subset $^k\mathcal{N}^e$ (lemma 4.15) on which we are to calculate the parities and delays (theorem 4.6).

Fragmentation of a node set   Let us call this division of odd set into smaller odd and even subsets the *partial fragmentation* f_1 of $^{k-1}\mathcal{N}^o$. We can apply another partial fragmentation f_2 of $^k\mathcal{N}^e$ into 2 odd subsets $\mathcal{F}_k' = \{^k\mathcal{N}_1^o, \, ^k\mathcal{N}_2^o\}$, and call the 2 fragmentations f_1, f_2 of $^k\mathcal{N}^o$ into a set of node sets $\mathcal{F}_k = \{^1\mathcal{N}_0^o, \, ^1\mathcal{N}_1^o, \, ^1\mathcal{N}_2^o\}$ a *fragmentation step* f. Each odd subset $^k\mathcal{N}_i^o$ of $\mathcal{F}_k$ can continue to be partially fragmented by f_1 into $^{k+1}\mathcal{N}_{i,0}^{o,o}$ and $^{k+1}\mathcal{N}_i^{o,e}$ the same way. Note that a node set $\mathcal{N}^o$ can only be fragmented if $S_{\mathcal{N}^o} \geq 3$, in which case the resulting subsets have size 1.

Lemma 4.17 *Let the separation of an odd node set $^{k-1}\mathcal{N}^o$ into subsets $\mathcal{F}_k' = \{^k\mathcal{N}_0^o, \, ^k\mathcal{N}^e\}$ be the partial fragmentation f_1 and subsequently into subsets $\mathcal{F}_k = \{^k\mathcal{N}_0^o, \, ^k\mathcal{N}_1^o, \, ^k\mathcal{N}_2^o\}$ be f_2 of $\mathcal{N}$. The combination of the two is a fragmentation step f.*

$$\mathcal{F}_k = f(^{k-1}\mathcal{N}^o) = f_2(f_1(^{k-1}\mathcal{N}^o)) = f_2(\{^k\mathcal{N}_0^o, \, ^k\mathcal{N}^e\}) = \{^k\mathcal{N}_0^o, \, ^k\mathcal{N}_1^o, \, ^k\mathcal{N}_2^o\} \quad | \quad S_{^k\mathcal{N}_i^o} \geq 3 \tag{4.9}$$

Each odd node set of $\mathcal{F}_k$ can undergo the same fragmentation step into odd subsets, leaving us again with a set of node subsets $\mathcal{F}_{k+1}$. We can do this some p times until our resulting set of node sets $\mathcal{F}_p$ consists only of smallest possible node subsets $\mathcal{N}^o$ where $S_{\mathcal{N}^o} = 1$. To find the worst case complexity, we want to maximize the delay complexity within $^{k-1}\mathcal{N}^o$; we are to find the sequence of joint operations that maximizes the sum of even node sets sizes $S_{\mathcal{N}^e}$ in all partial fragmentations in the *full fragmentation* F of $\mathcal{N}^o$.

Looking at the fragmentation from the other way, we have a set of size 1 node sets that undergo joint operations in each partial fragmentation. In f_2, two odd node sets join, and we do not add to the count of N_delay. In f_1, an odd and an even note sets join, and we have to calculate the delays in the even node set before moving on to the next joint operation.

Lemma 4.18 *Let the full fragmentation of $\mathcal{N}$ be*

$$F(\mathcal{N}^o) = \underbrace{f(f(...f(\mathcal{N})))}_{p \; times} = \{^p\mathcal{N}_1^o, \, ^p\mathcal{N}_1^o, \, ^p\mathcal{N}_2^o, ..., \, ^p\mathcal{N}_{N_\sigma}^o\} \quad | \quad S_{^p\mathcal{N}_i^o} = 1, \tag{4.10}$$

where along each fragmentation step k a partial fragmentation set $\mathcal{F}_k'$ is produced, the number of delay calculations is

$$N_{delay} = \sum_{k=1}^{p} \sum \{S_{^k\mathcal{N}^e} | \forall \; even \; ^k\mathcal{N}^e \in \mathcal{F}_k'\}. \tag{4.11}$$

Partial fragmentation number Note that here we ignore the fact that the partial fragmentations of some node set may not result in two but many subsets. Let us call the number of odd subsets the *fragmentation number* N_f. For partial fragmentation f_1, the separation of the odd node set $^{k-1}\mathcal{N}^o$ must be in 1 odd and 1 even subset per lemma 4.15, thus $N_{f_1} = 2$. For partial fragmentation f_2, the separation of even set $^k\mathcal{N}^e$ can be in $2n_o$ odd and n_e even subsets. But any even subset will be subjected to the same partial fragmentation f_2 in the full fragmentation, reducing the fragmentation number to $N_{f_2} = 2n_o$.

To find N_{f_2}, let us consider two cases where $n_o = 1$ or $n_o = 2$. If an even node set $\mathcal{N}^e$ is fragmented with $^k N_{f_2} = 2$, a fragmentation step of f_2, f_1 will be

$$\begin{aligned}
\mathcal{F}_k^e &= \{^k\mathcal{N}_1^o, {}^k\mathcal{N}_2^o\}, \\
\mathcal{F}_{k+1}'^e &= \{^{k+1}\mathcal{N}_{1,0}^{o,o}, {}^{k+1}\mathcal{N}_1^{o,e}, {}^{k+1}\mathcal{N}_{2,0}^{o,o}, {}^{k+1}\mathcal{N}_2^{o,e}\}.
\end{aligned}$$

For $N_{f_2} = 4$, a fragmentation step will be

$$\begin{aligned}
\mathcal{F}_k^e &= \{^k\mathcal{N}_1^o, {}^k\mathcal{N}_2^o \, {}^k\mathcal{N}_3^o \, {}^k\mathcal{N}_4^o\}, \\
\mathcal{F}_{k+1}'^e &= \{^{k+1}\mathcal{N}_{1,0}^{o,o}, {}^{k+1}\mathcal{N}_1^{o,e}, {}^{k+1}\mathcal{N}_{2,0}^{o,o}, {}^{k+1}\mathcal{N}_2^{o,e}, {}^{k+1}\mathcal{N}_{3,0}^{o,o}, {}^{k+1}\mathcal{N}_3^{o,e}, {}^{k+1}\mathcal{N}_{4,0}^{o,o}, {}^{k+1}\mathcal{N}_4^{o,e}\}.
\end{aligned}$$

If the size of $S_{\mathcal{N}^e}$ is large enough, and we fragment in the same ratio (see next paragraph), the sum of even node set sizes in these two kinds of fragmentations will be the same. However, the number of subsets in each fragmentation step has increased by a factor of 2, which means that the average size of subsets have decreased by 2. Consequently, the node set size decreases faster towards the minimum size of 3 as more fragmentation steps are applied. As the sum of even node set sizes in each fragmentation step is the same, increasing N_{f_2} will decrease the number of fragmentation steps and thus the number of delay calculations N_{delay} per equation 4.11. Thus our decision of $N_{f_2} = 2$ in lemma 4.17 is correct.

Partial fragmentation ratio To complete the fragmentation description, we will need to find the fragmentation ratios R_0, R_1, R_2 of a fragmentation step. The fragmentation ratios determine the node set sizes of the subsets in $\mathcal{F}_{k-1}$ with respect to the size of $^k\mathcal{N}^o$, where $R_i S_{k-1\mathcal{N}^o}$ is the size of subset $^k\mathcal{N}_i^o$. Note that R_0 corresponds to the odd subset from f_1, and R_1, R_2 to the odd subsets in f_2.

Lemma 4.19 *Let the fragmentation ratios R_0, R_2, R_2 be the relative set sizes of the odd subsets in the fragmentation set $\mathcal{F}_k = \{^k\mathcal{N}_0^o, {}^k\mathcal{N}_1^o, {}^k\mathcal{N}_2^o\}$ with respect to set $^{k-1}\mathcal{N}^o$, where*

$$R_j = \frac{S_{k\mathcal{N}_j^o}}{S_{k-1\mathcal{N}^o}} \tag{4.12}$$

Recall lemma 4.16 that the delay calculations are only done before a cluster is grown. During this grow process, some n_v vertices are added to the cluster, and some union or joint

operations can occur. If no joint operations occur, the node set stays unchanged, and the cluster is allowed to continue growth without delay calculations per lemma 4.12. We want to minimize n_v, as each added vertex here is not a node that can possibly count towards N_{delay}, and it is therefore preferable that some joint operations do occur during growth.

Take the first fragmentation sets $\mathcal{F}'_k = \{\mathcal{N}^o_0, \mathcal{N}^e\}$ and $\mathcal{F}_k = \{\mathcal{N}^o_0, \mathcal{N}^o_1, \mathcal{N}^o_2\}$ of some cluster defined by node set $^{k-1}\mathcal{N}^o$. These partial fragmentation correspond to 2 joint operations, between two odd clusters $\mathcal{N}^o_1, \mathcal{N}^o_2$ in f_2, and between odd and even clusters $\mathcal{N}^o_0, \mathcal{N}^e$ in f_1.

If we want to minimize n_v in f_2, these odd clusters must grow within the same bucket b_i, which means that $S_{\mathcal{V}_1} = S_{\mathcal{V}_2}$. Note that these are the cluster sizes and not node set sizes. For f_1, the joint event is caused by growth of $\mathcal{N}^o_0$ in either some bucket $b_j > b_i$ where $S_{\mathcal{V}_0} > S_{\mathcal{V}_1}$, or growth in the same bucket b_i where $S_{\mathcal{V}_0} = S_{\mathcal{V}_1}$. This leaves us with $S_{\mathcal{V}_0} \geq S_{\mathcal{V}_1} = S_{\mathcal{V}_2}$.

To maximize N_{delay}, we want to maximize $S_{\mathcal{N}^e} = S_{\mathcal{N}^o_1} + S_{\mathcal{N}^o_2}$ in f_1. Recall from equation ?? that $S_{\mathcal{N}} \leq S_{\mathcal{V}}$. We assume the largest possible node set size $S_{\mathcal{N}} = S_{\mathcal{V}}$ to find that $S_{\mathcal{N}^e}$ is largest if $S_{\mathcal{V}_0} = S_{\mathcal{V}_1}$. We can therefore conclude that $S_{\mathcal{N}^o_0} = S_{\mathcal{N}^o_1} = S_{\mathcal{N}^o_2}$ and $R_0 = R_1 = R_2 = \frac{1}{3}$

Lemma 4.20 *A fragmentation step of $^{k-1}\mathcal{N}^o$ is maximized in $S_{k\mathcal{N}^e}$ if the fragmentation ratios take the values $R_j = \frac{1}{3}$.*

Time complexity To find the time complexity cased by the delay calculations, we are left with a single variable p, the number of fragmentation steps that can be taken. If we assume that in each growth step not a single non-node vertex is added $n_v = 0$, the full fragmentation of some node set $\mathcal{N}^o$ is just the continuous division of the set in 3 parts per lemma 4.20, which can be calculated easily.

$$p = \log_3(S_{\mathcal{N}^o}) \tag{4.13}$$

In each fragmentation step $\mathcal{F}'_k$, f_1 is equivalent to the joint of odd node sets with even node sets where the sum of odd sets sizes is

$$\sum \{S_{k\mathcal{N}^o} | \forall \text{ odd } {}^k\mathcal{N}^o \in \mathcal{F}'_k\} = \frac{1}{3} S_{\mathcal{N}^o}, \tag{4.14}$$

and the sum of even node set of sizes is

$$\sum \{S_{k\mathcal{N}^e} | \forall \text{ even } {}^k\mathcal{N}^e \in \mathcal{F}'_k\} = \frac{2}{3} S_{\mathcal{N}^o}. \tag{4.15}$$

This approximation is true as we have taken $S_{\mathcal{N}} = S_{\mathcal{V}}$ and $n_v = 0$. Filling in equation 4.13 and 4.15 in 4.11, we find that

$$\begin{aligned} N_{delay} &\leq \sum_{k=1}^{p} \sum \{S_{k\mathcal{N}^e} | \forall \text{ even } {}^{k}\mathcal{N}^e \in \mathcal{F}'_k\}. \\ &= \sum_{k=1}^{\log_3(S_{\mathcal{N}^o})} \frac{2}{3} S_{\mathcal{N}^o} \\ &= \frac{2}{3} S_{\mathcal{N}^o} \log_3(S_{\mathcal{N}^o}) \end{aligned} \tag{4.16}$$

The node set size of set $\mathcal{N}^o$ is bounded by the lattice size N. The worst case time complexity of the delay computation is bounded by $\mathcal{O}(N \log_3(N))$. The real worst-case complexity is even lower as it is quite certain that not all vertices are nodes such that $S_{\mathcal{N}} < S_{\mathcal{V}}$ and $n_v > 0$.

Bloom complexity

To grow a cluster represented by a node set $\mathcal{N}$, we have to traverse the entire set from root to stem to iterate over each boundary list that are stored at the nodes. Let's call the total number of times any node is traversed by `Bloom` N_{bloom}.

Similar to the previous section we make the assumption of a maximum number of nodes on the lattice where in each cluster $S_{\mathcal{N}} = S_{\mathcal{V}}$ and $n_v = 0$. Recall that every odd node set ${}^{k}N_i^o$ in each fragmentation set $\mathcal{F}_k$ is subjected to growth in each partial fragmentation, and that we start out with a maximum number of smallest cluster of size $S_{p\mathcal{N}} = S_{p\mathcal{V}} = 1$. Thus we are certain that with this assumption we have the upper bound in N_{bloom}.

$$N_{bloom} \leq \sum_{p}^{k=1} \sum \{S_{k\mathcal{N}} | {}^{k}\mathcal{N} \in \mathcal{F}_k\} \tag{4.17}$$

For a full fragmentation of $\mathcal{N}$ of size $S_{\mathcal{N}}$, the sum of all set sizes in each fragmentation set $\mathcal{F}$ is

$$\sum \{S_{k\mathcal{N}} | {}^{k}\mathcal{N} \in \mathcal{F}_k\} = S_{\mathcal{N}}. \tag{4.18}$$

By filling in p we find that

$$\begin{aligned} N_{bloom} &\leq \sum_{p}^{k=1} \sum \{S_{k\mathcal{N}} | {}^{k}\mathcal{N} \in \mathcal{F}_k\} \\ &= \sum_{k=1}^{\log_3(S_{\mathcal{N}^o})} S_{\mathcal{N}} \\ &= S_{\mathcal{N}^o} \log_3(S_{\mathcal{N}^o}), \end{aligned} \tag{4.19}$$

which again corresponds to a worst case time complexity that is bounded by $\mathcal{O}(N \log_3(N))$.

4.5.9   Boundaries

4.5.10   Erasure noise

Chapter 5

Threshold simulations

To test for the threshold Pauli error value, we simulate for a large number of samples at various lattice sizes for a range of Pauli error rates around $p = 0.1$. For the threshold, only Pauli X errors are considered, as Pauli Z errors will give the same result. For each lattice size and Pauli error rate, the samples will return a probability rate of successful decodings P_{succes}. We will then fit the data to the function ([**?**], equation 43):

$$P_{succes} = A + Bx + Cx^2 + \begin{cases} D_{even} \cdot L^{-1/\mu_{even}} & \text{L even} \\ D_{odd} \cdot L^{-1/\mu_{odd}} & \text{L odd} \end{cases} \tag{5.1}$$

$$\text{with } x = (p - p_{thres})L^{1/\nu} \tag{5.2}$$

where all but P_{succes}, p and L are fitting parameters. Note that there are distinct values for D and μ for even and odd lattices. This is due to a discrepancy in the decoder threshold caused by a nonnegligible finite-size effect for even and odd lattices. Therefore, for each fit done on any dataset, only data from even or odd lattices will be selected. The fitting of the data will be done in Python using a least squared method.

Appendices

Appendix A

Bucket sort

Maximum number of growth iterations To categorize the clusters into buckets, we need to know how many buckets we would need. To find out, let us look at two generators that are placed maximally far from each other. On a even toric lattice with length l, they are placed $l/2$ horizontally and $l/2$ vertically from each other. If clusters from each bucket grow simultaneously by a half-edge, these two single-generator clusters would meet each other after l iterations, or including odd lattices, after $2\lfloor l/2 \rfloor$ iterations. As illustrated in figure A.1, we see that now the entire lattice is covered, thus this is exactly the number of iterations needed.

Lemma A.1 *Given a toric lattice with size $\{l, l\}$, a maximum number of $N_B = 2\lfloor l/2 \rfloor$ buckets is required for all generators to be connected, where clusters from each bucket is grown simultaneously.*
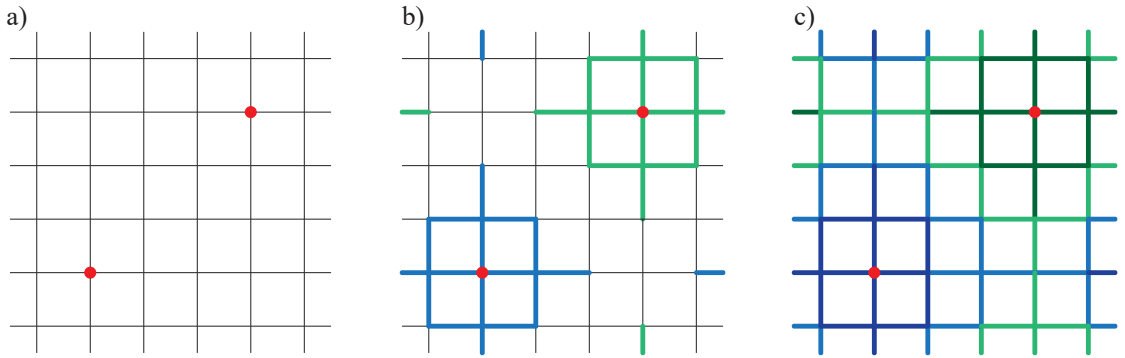

Figure A.1: If two single-generator clusters are placed a) maximally far from each other, b) a maximal number of growth iterations is needed. c) After $2\lfloor l/2 \rfloor$ iterations, the entire lattice is covered.

Analytical cluster categorization To sort or place the clusters into the buckets, we can again look at the case of the two generators. We presume that each growth iteration of the cluster is started from a different bucket. Knowing this, we can use the sequence of the size of the single-generator cluster as it grows.

$$S_{cluster,i} = 1, 1, 5, 5, 13, 13, 25, 25, 41, 41, 61, 61, ... \tag{A.1}$$

Note that a cluster does not increase in size in alternating iterations, as the growth of half-edges does not add new vertices to the cluster. We ignore these duplicate numbers for now. We find that this series of numbers can be written as a finite sum.

$$S'_{cluster}(i) = 1 + \sum_{0}^{x=i} 4x = 2i(i+1) + 1 \tag{A.2}$$

We now have a very simple analytical function to place clusters into buckets, where the number of elements per bucket increases linearly with $4i+8$. For a cluster of size S, its bucket number i can be calculated by rewriting and flooring equation A.2 $i = \lfloor (\sqrt{2S-1}-1)/2 \rfloor$. Now earlier we disregarded the duplicate entries is $S_{cluster,i}$, so we need to take an extra step to check whether a cluster is in its half-grown state. These buckets are illustrated in figure A.2a.

Definition A.1 (Bucket place method 1) *A cluster with size S is placed in bucket number i of l buckets with $i = 2\lfloor (\sqrt{2S-1}-1)/2 \rfloor$ if cluster is fully grown, or $i = 2\lfloor (\sqrt{2S-1}-1)/2 \rfloor + 1$ otherwise.*

a) place method A

1-4 full	1-4 half	5-12 full	5-12 half	13-24 full	13-24 half
0	**1**	**2**	**3**	**4**	**5**

● ● ●

b) place method B

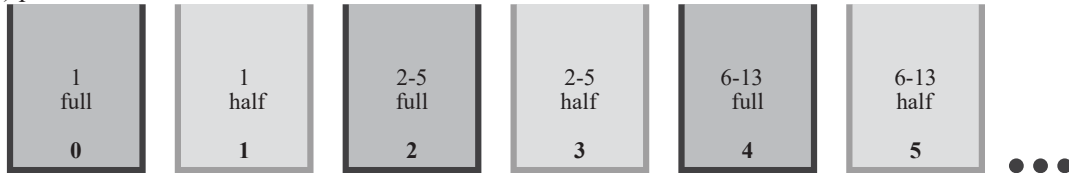| 1 full	1 half	2-5 full	2-5 half	6-13 full	6-13 half
0	**1**	**2**	**3**	**4**	**5**

● ● ●

Figure A.2: The first six buckets for a) method A from definition A.1 and b) method B from definition A.2. Even buckets contains fully grown clusters, odd buckets contain half-grown clusters of the same size.

Single-generator clusters, or clusters with size 1, is never caused by an only an erasure error. It might therefore by useful to give these clusters their own bucket, such that these single-generator clusters are always grown first, such as in figure A.2b.

Definition A.2 (Bucket place method 2) *For separate single-generator buckets, check whether the cluster has size 1, in which case the clusters belongs in bucket 0 or 1 depending on its growth state. Otherwise, a cluster with size S belongs in bucket number i of l buckets with $i = 2\lfloor(\sqrt{2S-3}-1)/2\rfloor + 1$ if cluster is fully grown, or $i = 2\lfloor(\sqrt{2S-3}-1)/2\rfloor + 2$ otherwise.*

To compare method 1 of definition A.1 and method 2 of definition A.2, let us find the size of the largest odd possible on a lattice. Given that any two odd parity clusters grow simultaneously, this size is $S_{max} = (\lfloor l/2 \rfloor - 1)l$. We calculate the bucket number (for the half-grown state) for both methods and plot them versus the lattice size in figure A.3. The bucket number of the largest odd parity cluster for method 2 is exactly the largest available bucket. Therefore method 2 is most probably superior.
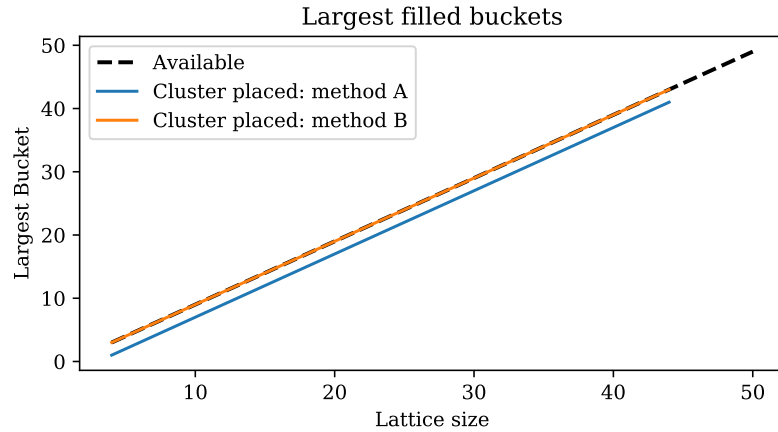

Figure A.3: The largest bucket that will be utilized for methods A and B (see fig. A.2). Method A does not utilize the largest two buckets.

The big benefit of this type of bucket sort is that we do not need to look at existing entries in the buckets. Only thing that is necessary is to initialize the buckets, which can be done in linear time.

Growing a bucket   The procedure for the Union-Find decoder using the bucket sort algorithm is now to sequentially grow the buckets starting from bucket 0, which contains all the single-generator clusters. From each bucket, which can be a simple list, clusters are popped from the bucket, grown, and placed into a new bucket, a process which we will call *growing a bucket*. In the case that no merge happens, clusters from even bucket i are placed in odd bucket $i + 1$. However, what happens to clusters grown from odd bucket j?

It would be problematic if a cluster can be placed in even bucket $j-1$, which has the same size range, as that bucket comes first in the sequence, and thus will not be grown again. To proof that this will never happen, let's state the following:

Lemma A.2 *A cluster with size $S_i = 2(i+1)(i+2) + 1$ grown from a single-generator cluster has the least number of neighbor vertices of all clusters of size S_i.*

This is equivalent to saying that single-generator seeded cluster with size S_i will have the least amount of new vertices added to itself for all clusters with the same size. This is fairly easy to proof, as there can be no more compactly organized cluster than a cluster grown from a single generator. We know odd parity clusters from this most compactly organized set must go into the next bucket, as the size of this set if clusters is what defines the sequence (eq. A.1). Thus less compactly organized odd parity clusters must at least grow into the next even bucket, and potentially grow into a higher even bucket.

Lemma A.3 *In the case of no merging event, clusters from even bucket i are grown into bucket $i+1$, and cluster from odd bucket j are grown into bucket $j + 2k + 1$ with $k \in \mathbb{N}_0$.*

We now know that our buckets can be grown sequentially, where we need not to worry about buckets that already been emptied.

Merging   Up until now we have avoided talking about the merging of clusters, so let us finally address this. In the original paper of the Union-Find algorithm, when two clusters merge, one needs to check for the larger cluster between the two, and make the smaller cluster the child of the bigger cluster, which lowers the depth of the tree and is called the *weighted union rule*. Applied to the toric lattice, the Union-Find decoder also needs to append the boundary list (which contains all the boundary edges of a cluster) of the smaller cluster onto the list of the larger cluster.

In our application, instead of appending the entire boundary list, we just add a pointer at the parent cluster to the child cluster. As a parent can have many children, the pointers are appended to a *children list*. When growing a cluster, we first check if this cluster has any child clusters. If yes, these child clusters will be grown first by popping them from the list, but any new vertices will always be added to the parent cluster. Also during and after a merge, we make sure that any new vertices are always added to the parent cluster. Any child will exist in the list of a parent for one iteration, after which its boundaries will be grown, and the child is absorbed into the parent. This method also works recursively by keeping track of the root cluster instead of the parent cluster, and many levels of parent-child relationships can exists.

Faulty entries   Now let us first be clear: *only uneven parity clusters will be placed in buckets, but each bucket does not only contain uneven parity clusters.* As a merge happens between two uneven parity clusters A and B during growth of B, cluster A has already been placed in a bucket. But clusters A is now part of cluster AB and is even. So, to prevent
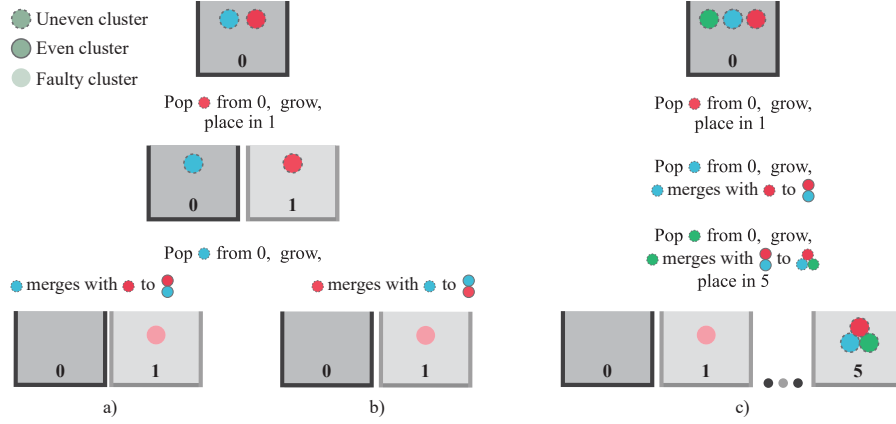
Figure A.4: bla

growth of the *faulty entry*, we just need to have an extra check of the parity of the root cluster.

Wastebasket   If the lattice consists of more than just the two single-generator clusters, it is entirely possible for odd parity clusters to grow larger than $S_{max} = (l/2 - 1)l$. The bucketing formulas also does not prevent itself from outputting a larger bucket number than the available number of buckets. The elegance of this method is that whenever a cluster has a bucket number $i_1 > l$, there will always be another *smaller* cluster with bucket number $i_2 \leq l$ that will merge into the larger cluster, which evens the parity. In another words, if a clusters bucket number i is computed to be larger than l, we can figuratively put the cluster into the *wastebasket*.

Bibliography

[1] CJ Ballance, TP Harty, NM Linke, MA Sepiol, and DM Lucas. High-fidelity quantum logic gates using trapped-ion hyperfine qubits. *Physical review letters*, 117(6):060504, 2016.

[2] A Robert Calderbank and Peter W Shor. Good quantum error-correcting codes exist. *Physical Review A*, 54(2):1098, 1996.

[3] Andrew Steane. Multiple-particle interference and quantum error correction. *Proceedings of the Royal Society of London. Series A: Mathematical, Physical and Engineering Sciences*, 452(1954):2551–2577, 1996.

[4] John Preskill. Reliable quantum computers. *Proceedings of the Royal Society of London. Series A: Mathematical, Physical and Engineering Sciences*, 454(1969):385–410, 1998.

[5] Daniel Gottesman. Stabilizer codes and quantum error correction, 1997.

[6] Raymond Laflamme, Cesar Miquel, Juan Pablo Paz, and Wojciech Hubert Zurek. Perfect quantum error correcting code. *Phys. Rev. Lett.*, 77:198–201, Jul 1996.

[7]

[8] Nicolas Delfosse and Gilles Zémor. Linear-time maximum likelihood decoding of surface codes over the quantum erasure channel. *arXiv preprint arXiv:1703.01517*, 2017.

[9] Nicolas Delfosse and Naomi H Nickerson. Almost-linear time decoding algorithm for topological codes. *arXiv preprint arXiv:1709.06218*, 2017.

[10] Robert Endre Tarjan. Efficiency of a good but not linear set union algorithm. *Journal of the ACM (JACM)*, 22(2):215–225, 1975.

[11] N. Leijenhorst. Quantum error correction, decoders for the toric code. Bachelor thesis, Delft University of Technology, July 2019. Applied Mathematics and Applied Physics BSc.